CONFIDENTIAL

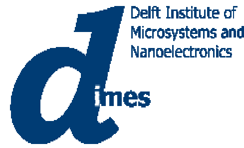

† Confidential

Electrical Characterization of MEMS Microphones

Gokulraj Chandramohan

Under the guidance of : Prof.dr.P.M.(Lina) Sarro
Electronic Components, Technology and Materials (ECTM)
Delft Institute of Microsystems and Nanoelectronics (DIMES)
Faculty of Electrical Engineering, Mathematics and Computer Science
Delft University of Technology, The Netherlands

Supervisors : Dr. Twan van Lippen, Dr. Klaus Reimann and Iris Bominaar-Silkens
Corporate I&T / Research
Microsystems Technology Group,
NXP Semiconductors, Eindhoven, The Netherlands

August 2010

Abstract

A reliable characterization of a MEMS microphone is essential for a better understanding of the device physics, for estimating the device performance and for guidance during the research, for better microphones. The work presented in this report focuses on the investigation and comparison of different measurement principles and techniques used to measure the key device parameters resonance frequency and compliance. The first generation MEMS microphones that are developed by NXP are influenced by mechanical vibrations that reduces the device performance. Therefore, new techniques will be implemented to reduce this noise and these techniques are based upon matching the frequencies of two flexible plates in the microphone sensor, we investigate these resonance frequencies in this thesis. This investigation is performed with two different measurement techniques : electrical impedance measurements and laser vibrometer experiments. These measurements are performed in air and vacuum conditions and the influence of ambient pressure, bias voltage and back volume on the resonance frequency is investigated. The vacuum measurements are in good agreement with the finite element simulation results. Additionally the results obtained from different measurements are compared and the difference between the results are analyzed. Finally, recommendations are made for future measurement conditions and setups.

Acknowledgement

I owe my great thanks to many people who helped and supported me during my thesis and graduate studies.

First I would like to thank Professor dr. Lina Sarro for giving me a wonderful opportunity to do my master thesis in collaboration with the Electronic Components, Technology and Materials (ECTM) group at TU Delft and the Microsystem Technology group of NXP Semiconductors, Eindhoven. I'm especially grateful for her support, thoughtful guidance and encouragement throughout my academic life in The Netherlands.

Secondly, my sincere thanks to dr. Twan Van Lippen, Iris Bominaar-Silkens and dr. Klaus Reimann for their constant support, encouragement and guidance in spite of their busy schedules. They were always available to resolve my doubts. Also I want to express my gratitude to Remco Pijnenburg and Mieke Botermans for their suggestions and comments during our bi-weekly meetings at NXP. Additionally my deepest thanks to dr. ir. Martijn Goossens for his constant help and patience in the measurement lab.

I would like to thank my friends Andrés Vásquez, Shuang Song, Onur Kaya, Mahidhar, Karthik, Venkatasubramaniam, Aditya, Aadithya, Rajat Bharatwaj, Madhavan, Shilesh, Chockalingam, Supriya, Vinoth and my house mates Santiago, Cesar, Eric Periot, Kevin Brands, Sundeep for their support and being there for me when I needed them most.

I would like to express my love to my parents Chandramohan and Umarani, and my sister Divya for giving me the freedom to dream and chase my dreams.

Finally my sincere and heartfelt thanks to the Almighty for all the shine of health and wealth bestowed upon me, throughout my life.

Contents

1 Introduction **5**
- 1.1 Motivation . . . 5
- 1.2 Objective . . . 7
- 1.3 Thesis Organization . . . 8

2 MEMS Microphone Concept **9**
- 2.1 MEMS Capacitive Microphones . . . 9
- 2.2 NXP MEMS Microphone . . . 10
  - 2.2.1 Microphone Sensitivity . . . 12
- 2.3 Body-Noise Cancellation . . . 13
  - 2.3.1 Frequency Matching . . . 15
- 2.4 Compliance . . . 18

3 Laser Vibrometer Measurement **19**
- 3.1 Measurement Setup . . . 19
- 3.2 Test Measurements . . . 23
  - 3.2.1 2X and 50X Magnification Measurement . . . 23
- 3.3 Backplate Frequency Measurement Results . . . 26
- 3.4 Measurement of membrane at Low Frequency . . . 27
  - 3.4.1 Wafer sample measurement . . . 27
  - 3.4.2 Packaged sample measurement . . . 28
- 3.5 Extraction of Electrostatic Force . . . 29
- 3.6 Summary . . . 29

4 Electrical Impedance Measurement **31**
- 4.1 Frequency Response Measurement . . . 31
  - 4.1.1 Measurement Set-ups . . . 32
  - 4.1.2 Measurement setup Calibration . . . 33
- 4.2 Resonance Frequency . . . 34
  - 4.2.1 Extraction of Resonance frequency . . . 36
  - 4.2.2 Air and Vacuum Measurement Results . . . 39
    - 4.2.2.1 Wafer and Packaged Sample Measurement Results 40
    - 4.2.2.2 Backplate resonance frequency and stress . . . 42
- 4.3 Capacitance – Voltage Measurement . . . 43
  - 4.3.1 Extraction of Membrane Compliance . . . 44
  - 4.3.2 Optimal Frequency selection . . . 47
  - 4.3.3 Influence of AC voltage . . . 48
  - 4.3.4 Membrane compliance in vacuum . . . 48

4.4 Summary 49

5 Measurement Results Comparison and Discussion 50

6 Conclusions and Recommendations 54
6.1 Conclusions 54
6.2 Recommendations 55

Bibliography 56

A Influence of calibration techniques on the extracted results 57

B 10 cycles with same conditions (2X) 59

List of Symbols

A_m	Area of membrane	[m^2]
a	Acceleration	[m/s^2]
C	Compliance	[m/N]
C_m	Membrane Compliance	[m/N]
C_{eff}	Effective Compliance	[m/N]
c	Speed of sound	[m/s]
C_s	Series Capacitance	[F]
C_0	Capacitance at 0V	[F]
C_P	Parasitic Capacitance	[F]
D	Dissipation Factor	[-]
F	Force	[N]
f_{res}	Resonance Frequency	[Hz]
F_e	Electrostatic Force	[N]
f_{00}	Fundamental Eigen mode frequency	[Hz]
g	Air Gap	[m]
h_m	Thickness of membrane	[m]
h_{bp}	Thickness of backplate	[m]
k	Spring Constant	[N/m]
k_{eff}	Effective Spring constant	[N/m]
k_{el}	Electrical Spring constant	[N/m]
M	Mass	[kg]
m_{eff}	Effective mass	[kg]
R_m	Radius of membrane	[m]
R_{bp}	Radius of backplate	[m]
S_e	Electrical Sensitivity	[V/Pa]
V_{bias}	Bias Voltage	[V]
$V_{pull-in}$	Pull-In Voltage	[V]
x	Displacement	[m]
ρ_a	Density of Air	[kg/m^3]
ε	Permittivity	[F/m]
ρ	Density of Silicon	[kg/m^3]
$\sigma_{f_{res}}$	Error in resonance frequency	[Hz]
ω'_{nm}	Eigen value	[-]
σ	Stress	[Pa]
σ_{C_m}	Error in membrane compliance	[m/N]

Chapter 1

Introduction

This chapter is structured into three sections. The first two sections focus on the project's motivation and the objectives of the work. The final topic gives an overview about the organization of this report.

1.1 Motivation

Humans have always tried to extend their capabilities. Firstly, they extended their mechanical powers. They invented the steam engine, the combustion engine, the electric motor and the jet engine. Mechanization thoroughly changed society. Secondly, they extended their brains. They invented means for artificial logic and communication: the computer and the internet. This information phase is changing society again, where we cannot yet fully predict the end result. However, this is not all. By inventing sensors, humans are now learning to artificially expand their senses. Sensorization together with mechanization and informatization will bring about the third industrial revolution [1].

Sensors transform signals from different energy domains to the electrical domain. Fig. 1.1 shows the different signal domains[2].

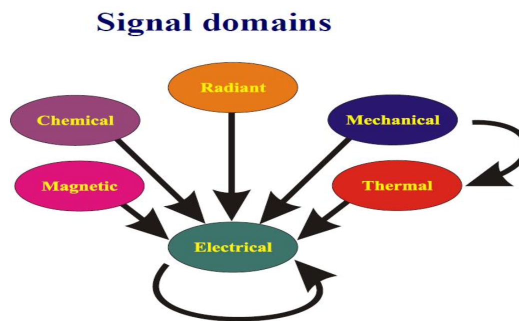

Figure 1.1: Sensor Classification according to six signal domains[2]

This figure explains the conversion from different signal domains into the electrical domain. In our case, for example, the microphone converts the acoustic

sound, which is a mechanical signal, into an electrical signal by using capacitive principle.

There is always a need for improvement and the demand for faster, cheaper, more reliable quality products. Our thesis deals with NXP MEMS (Micro Electro Mechanical Systems) microphones. Nowadays microphones are present in all electronic gadgets such as mobile phones, personal digital assistants (PDA), digital cameras and camcorders. This provides a big market space for the microphone business (Fig.1.2).

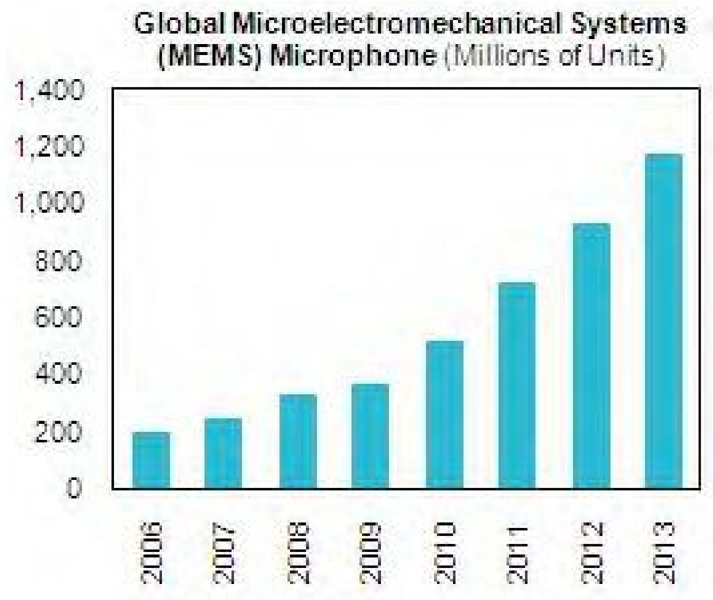

Figure 1.2: MEMS Microphones market prediction[3]

NXP produces microphones and speakers for mobile phones. In order to give the customers the best in technology microphones, NXP chooses to use MEMS technology based capacitive microphones. Other microphones used are conventional condenser or electret microphones, piezoelectric, piezoresistive, magnetic or optical microphones [4]. Out of these, the most commonly used microphones are condenser microphones consisting of a flexible diaphragm and a rigid counter electrode. The diaphragm acts as one plate of capacitor, and the sound vibrations produce changes in the capacitance between the plates. The most popular microphones used in most of the present electronic devices are the electret microphones. It is expected that the electret microphones will soon be replaced by the MEMS based microphones [5].

The advantages of MEMS microphones are their reproducibility, smaller size, integration with electronic circuitry in the same package, volume production and automated pick-and-place compatibility. When considering MEMS microphones in mobile phones they have several functional advantages like improved sound quality, greater range and smaller size [6] which leaves space for other MEMS devices such as gyroscopes and accelerometers. These advantages made NXP

to opt for the MEMS microphones.

NXP has developed the first generation microphone sensor and wants to improve its performance for better sensitivity and less noise. To accomplish those tasks, research has to be done to understand the device characteristics and to come up with solutions to reduce the noise.

1.2 Objective

The NXP microphone is a parallel plate capacitive microphone and its simple structure is shown in Fig.1.3. The main components of a MEMS capacitive microphone are a thin conductive membrane and a thick perforated conductive backplate, separated by an air gap. Hence, the plates form a parallel plate capacitor. These plates are biased with a constant charge Q.

The operation of the sensor is based on the capacitive principle. When the sound vibrates the membrane, it changes the distance between the plates. Therefore, the capacitance changes, which is translated into an electrical signal. The sensor is sealed by a back chamber so that sound can only reach one side of the membrane.

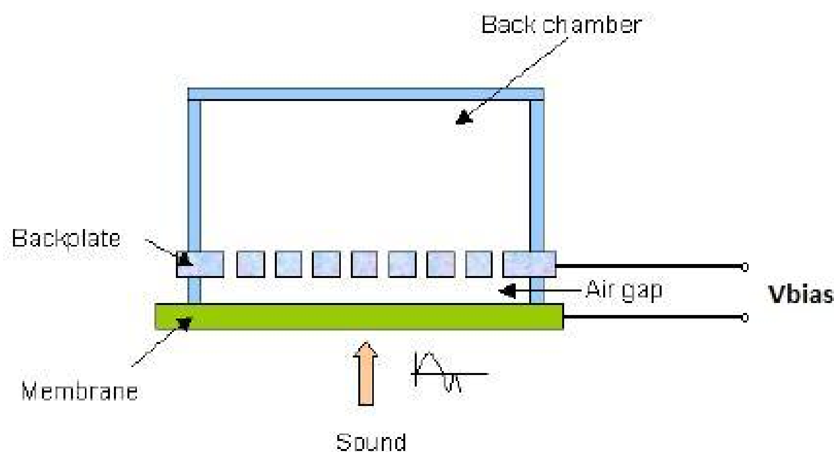

Figure 1.3: MEMS Capacitive microphone[7]

The current NXP MEMS microphones are subject to body-noise, which is the noise signal generated by the external mechanical vibrations. The desired behavior of the microphone is to be sensitive for sound only, but body noise implies that the microphone is sensitive for both sound and acceleration. Therefore, new techniques will be implemented in the next generation sensor to cancel this body-noise. One such technique is intrinsic compensation, which is also known as frequency matching.

Frequency matching is the technique that cancels the body-noise by matching the resonance frequencies of membrane and backplate. This can be realized by the present MEMS technology. The matching is achieved by making the backplate more flexible, so that its resonance frequency shifts closer to the membrane resonance frequency. When the resonance frequencies are matched, both

the membrane and backplate exhibit equal deflection for mechanical vibrations, thus avoiding the noise output.

Therefore, the main topic of this thesis is to investigate the resonance frequency of both membrane and backplate. Furthermore, we study the membrane compliance. The compliance is directly related to the sensitivity of the microphone sensor.

Different measurement principles are applied and compared. As it is known that the resonance frequency of the membrane depends on the bias voltage, air damping and back-volume. We investigated the influence of ambient pressure, bias voltage and back volume on the resonance frequency.

1.3 Thesis Organization

The theory and background information necessary to understand this thesis is given in chapter 2. Furthermore, we explain body noise and discuss the operating principle of the MEMS capacitive microphone.

In chapter 3 the laser vibrometer technique is discussed, along with the key results obtained from the measurement. Chapter 4 is completely focused on the electrical impedance measurements, their setups and the results obtained. Chapter 5 is dedicated to comparing the different measurement principles and results. Finally, Chapter 6 concludes with suggestions for future work and recommendations.

Chapter 2

MEMS Microphone Concept

This chapter focuses on the theory and information necessary to understand the work done in this thesis. First an introduction about the NXP MEMS microphone, its structure and operating principle is described. Then the body-noise problem is introduced with the possible measures to avoid it.

2.1 MEMS Capacitive Microphones

A microphone is an acoustic-to-electric transducer that converts sound into an electrical signal. Our main topic of interest is on MEMS capacitive microphones; MEMS (Micro Electro Mechanical Systems) are made up of components between 1 to 100 micrometers in size. The main purpose of MEMS is to use semiconductor fabrication technologies and processes to manufacture miniature mechanical elements which can be used as sensors and actuators on a silicon substrate [8]. Both the electrical and mechanical components can be combined to build an electro-mechanical system with a specific functionality. MEMS fabrication uses the integrated circuit batch processing technology for mass manufacturing and low device costs, additionally allowing system-on-chip options. Fig.2.1 shows a complicated MEMS device "A Ratchet" with dimensions in micrometer range.

A MEMS capacitive microphone combines both MEMS mechanical characteristics and capacitive microphone's characteristics. In general, a capacitive microphone consists of a flexible plate, named membrane, and a perforated rigid plate named backplate, separated by an air gap. Fig.2.2 shows the MEMS microphone operating principle. The membrane and backplate act as parallel plates of a capacitor and the air in-between the plates provides the dielectric of the capacitor. The back chamber is necessary to make sure that the sound reaches the membrane only from one side. This back chamber must be large enough to let the membrane move freely. The membrane is sensitive to acoustic pressure, and thus vibrates for the incoming acoustic signal. The backplate is perforated and thus allows the airflow to pass through. Hence the backplate is insensitive to the acoustic signal. The movement of the membrane changes the capacitance between the plates. This can be translated into electrical signal through the external circuitry.

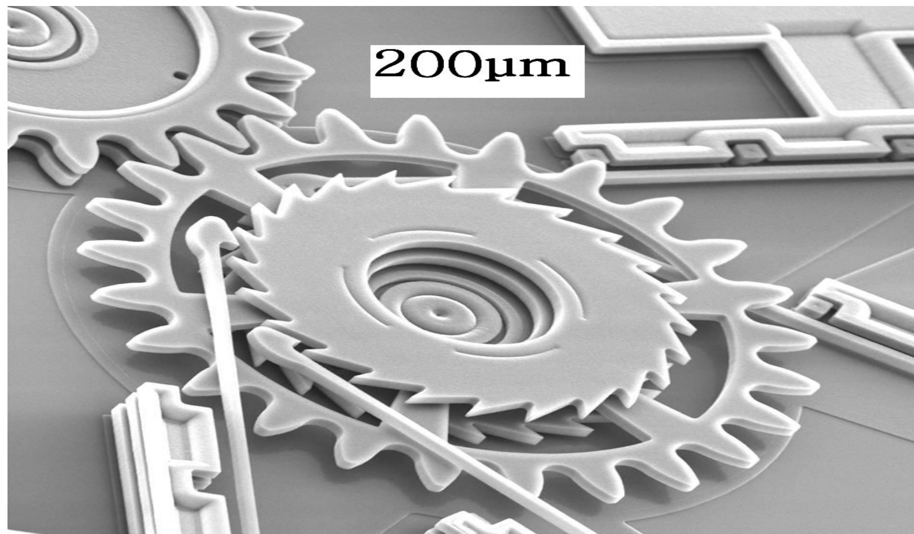

Figure 2.1: MEMS realization of mechanical component “A Ratchet”[9]

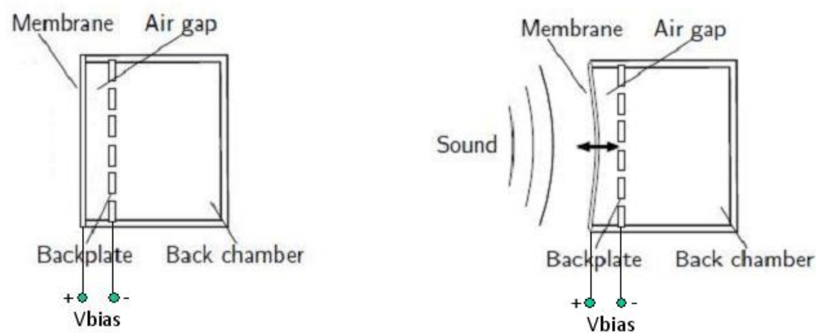

Figure 2.2: Capacitive microphone cross sectional view and its operation[10]

2.2 NXP MEMS Microphone

The MEMS microphone developed by NXP Semiconductors is based on the capacitive microphone principle. The cross section view of the NXP MEMS microphone with its dimensions is shown in Fig.2.3. Fig.2.4 shows the MEMS microphone in the wafer. The four contact pads are connected to the backplate, membrane and the substrate (2X).

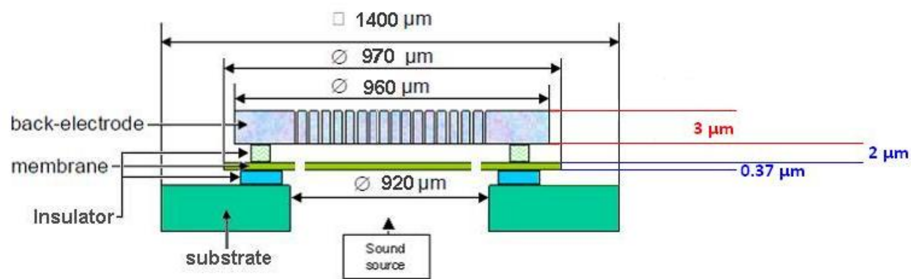

Figure 2.3: NXP MEMS microphone cross section of the device with dimensions

(a)

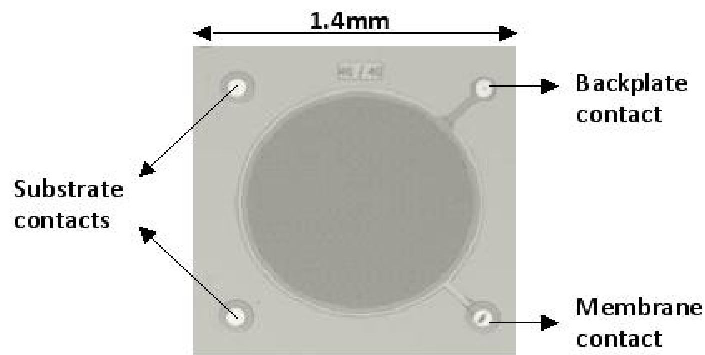

(b)

Figure 2.4: NXP MEMS microphones in (a) on a wafer. (b) Single device

The packaged NXP MEMS microphone is shown in Fig.2.5. It is packaged in a case of 4.72 mm x 3.76 mm x 1.1 mm with an opening for sound in the bottom. The Application Specific Integrated Circuit (ASIC) for the read-out of the audio signal is placed inside the same package. There are advantages and disadvantages of this package. The disadvantage is that the air inside the package will damp the moving membrane. The metal cap defines the back volume and in principle an infinite back volume is required for maximum sensitivity, which means no metal cap. In reality that is not possible since no back chamber means no reference pressure, so then the microphone cannot operate. Also the package is necessary to protect the device from rough environments in the real working environments.

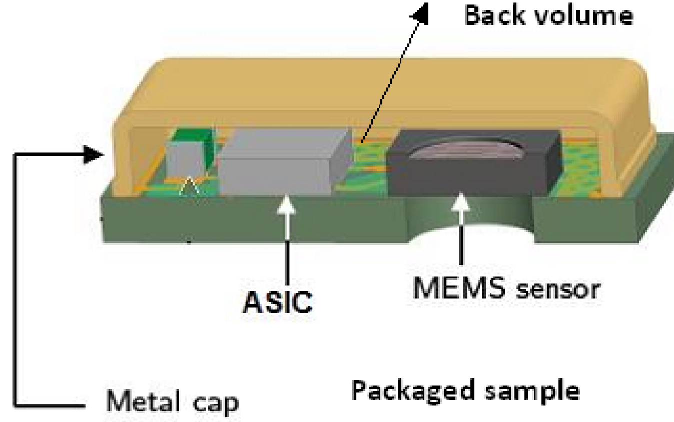

Figure 2.5: Packaged NXP MEMS microphone

2.2.1 Microphone Sensitivity

Before getting into the discussion of electrical sensitivity we will introduce the term called compliance. The elastic behavior of membrane is commonly quantified by this term instead of spring constant . The compliance (C) provides a measure of flexibility of the membrane and it is expressed as

$$C = \frac{1}{k} \tag{2.1}$$

where k is the spring constant in N/m. Hence, the unit of compliance is m/N.

The equation that describes the electrical sensitivity of the membrane is given by [11],

$$S_e = A_m C_{eff} \frac{V_{bias}}{g} \tag{2.2}$$

where S_e denotes the Electrical sensitivity, C_{eff} the effective compliance and A_m the area of membrane. V_{bias} is the bias voltage of the device and g is the distance between the membrane and backplate, also known as the air-gap thickness.

The effective compliance of the membrane depends on the mechanical membrane compliance extracted from C-V measurement $C_{m,cv}$, the back volume compliance C_{bv}

$$C_{bv} = \frac{V_{bv}}{\rho_a c^2 A_m^2} \tag{2.3}$$

and the electrical spring softening compliance $C_{kt,el}$:

$$C_{kt,el} = \frac{2g^3}{\varepsilon \pi R_m^2 V_{bias}^2} \tag{2.4}$$

C_{eff} depends on these terms according to :

$$\frac{1}{C_{eff}} = \frac{1}{C_{m,CV}} + \frac{1}{C_{bv}} - \frac{1}{C_{kt,el}} \tag{2.5}$$

where V_{bv} – Back volume, c – Speed of sound, ρ_a – Density of air, R_m- radius of membrane, ε- permittivity in F/m.

The spring softening compliance is negative since it opposes the spring restoring force. The equations describe how the membrane compliance and the back volume influence the sensitivity of the device. The back volume reduces the membrane movement which will affect the device performance. Therefore an optimal back volume for better performance has to be identified. Thus the measurement of membrane compliance and the analysis of back volume effects are necessary.

From Eqn.2.2 it is clear that the sensitivity depends on different parameters such as area of the membrane, effective compliance, bias voltage and the air gap. Therefore it is always a trade off between these terms to get the maximum sensitivity. For example, increasing the area of membrane in order to enhance the sensitivity is limited by the desired small device dimensions.

2.3 Body-Noise Cancellation

Body-noise is the undesired effect of a MEMS microphone to behave as an accelerometer. In other words, body-noise means that structure-borne sound is converted by the microphone into an electrical output, which cannot be distinguished by the receiver from the sound signal. Body-noise is a performance-limiting factor of microphones in a vibration environment. Body movement due to external vibrations is compared with normal operation in Fig.2.6.

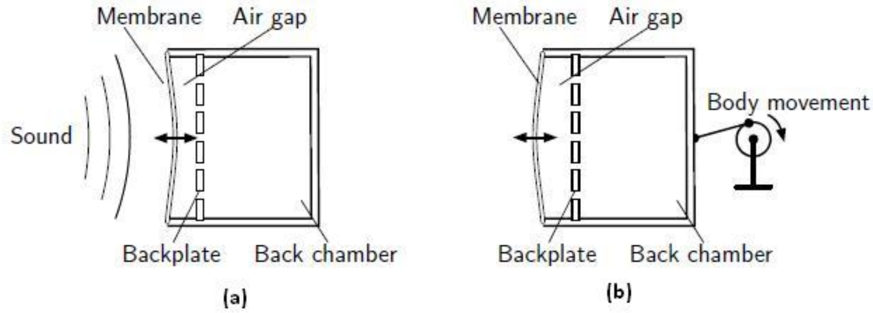

Figure 2.6: Body movement in comparison with normal operation[10]

Fig.2.6 (a) shows the normal operation of the microphone for the acoustic signal. In Fig.2.6 (b) the movement of membrane due to external mechanical vibrations can be identified. This movement causes the microphone membrane to vibrate, so that the capacitance between the plates changes. This change in capacitance produces a noise signal, which affects the performance of the microphone. Potential sources of body-noise are the vibrations in the environment, such as a working machine where the microphone is mounted or the propagation of sound of the speaker through the mobile phone circuits. The operational frequency range of the microphone is from 20Hz to 20kHz. This is well above the frequency (12Hz) of the vibrations produced by human body, so human-body movements are not important since they are intrinsically filtered [10].

NXP came up with several techniques to cancel this body noise [12]. At present, two methods are under consideration :

1. An intrinsic solution, based on matching the frequency response of the backplate to that of the membrane. This technique is called frequency matching. It will be discussed in detail in the next subsection.

2. The second method uses a separate accelerometer, placed next to the microphone sensor. This accelerometer acts as a deaf microphone, which senses only the body-noise signals [12]. The output of the accelerometer is subtracted from the output of the microphone. The accelerometer can be integrated in the same wafer as the microphone. The advantage of this technique is that the final device can be used as a microphone as well as an accelerometer, offering an additional functionality for mobile devices.

2.3.1 Frequency Matching

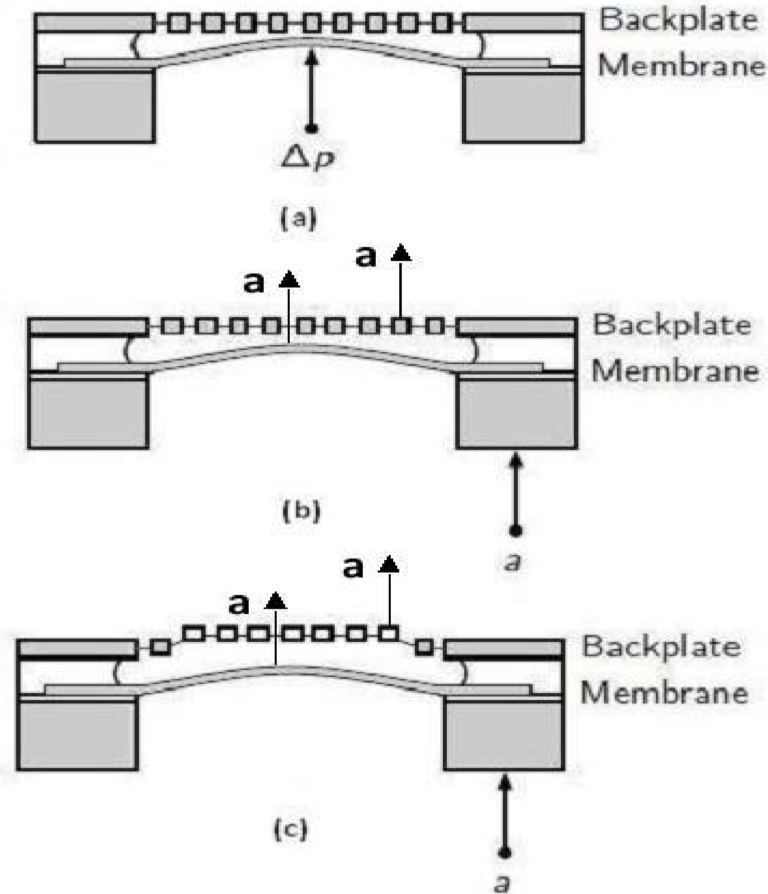

Figure 2.7: Frequency matching technique (a) Acoustic signal membrane movement (b) For acceleration signal membrane moves much more than the backplate (No Frequency matching) (C) After frequency matching both membrane and backplate move similarly in response to an external acceleration.

The intrinsic solution thus removes the body noise by making the backplate equally sensitive for the mechanical vibrations as the membrane. In other words, it is to match the membrane and backplate movement for the mechanical vibrations. This way, both backplate and membrane deflect the same when mechanically actuated, making the capacitance constant due to external vibrations. Since the backplate is perforated it is not sensitive for the acoustic signal so that the microphone is still sensitive to sound. We visualized the body noise cancellation procedure in Fig.2.7.

Fig.2.7(a) shows the normal operation of the device for acoustic signal where the membrane moves and the backplate not. In Fig.2.7(b) the membrane moves much more than the backplate due to the external acceleration as the membrane

is much more flexible than the backplate. Hence the body noise is generated. Fig.2.7(c) shows that after frequency matching the backplate is moving similarly to the membrane due to the external acceleration, thus avoiding the noise signal.

Hence, the backplate has to be designed in such a way that it is as sensitive to the external acceleration as the membrane. This can be explained in a simple approach. The membrane and backplate can be represented as a spring-mass system with a mass 'M' and a spring constant 'k' for the external acceleration as illustrated in Fig.2.8.

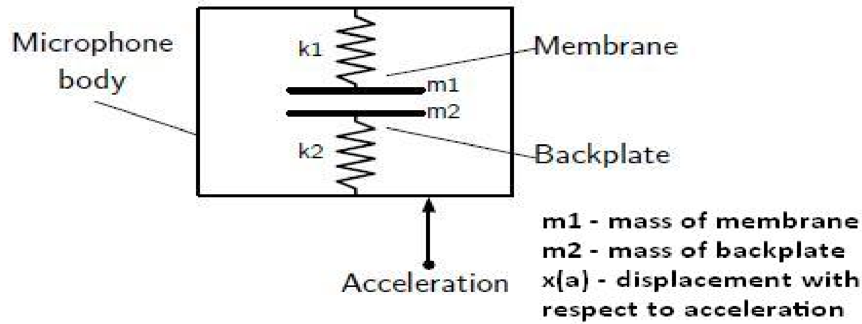

Figure 2.8: Mechanical model of the sensor for body acceleration[11]

Consider two simple mechanical formula's, the first being Newton's second law of motion

$$F = M * a \tag{2.6}$$

with F the force on the mass, M the mass and a the acceleration. The second equation is Hooke's law

$$F = k * x \tag{2.7}$$

for an extension x of the spring due to a force F with k the spring constant. When a mass is connected to a spring, these two forces are equal and we find

$$F = k * x = M * a$$

$$x(a) = \frac{M}{k} * a \tag{2.8}$$

stating that the displacement of the mass (or the extension of the spring) is proportional to the applied acceleration a. The proportionality is given by the spring constant k and the mass M.

The displacement 'x' of the mass due to acceleration 'a' has a sensitivity

$$\frac{dx}{da} = \frac{M}{k}$$

according to Eqn.2.8. This expression is valid for a static situation, i.e. for frequencies considerably below the fundamental resonance frequency of the system. The same ratio M/k appears in the resonance frequency (f_{res}) of the spring mass system :

$$f_{res} = \frac{1}{2\pi}\sqrt{\frac{k}{M}} \tag{2.9}$$

Therefore, we may conclude that the sensitivity to acceleration, $\frac{dx}{da}$, and the resonance frequency (f_{res}) are coupled inherently. By reducing the resonance frequency, we can thus improve the sensitivity to acceleration.

From Eqn.2.8 and Eqn.2.9 it follows that if the ratio $\frac{M}{k}$ is equal for both membrane and backplate, the displacement due to acceleration will be equal. This is exactly the desired behavior. Hence, body-noise compensation can be achieved by matching the resonance frequencies of membrane and backplate.

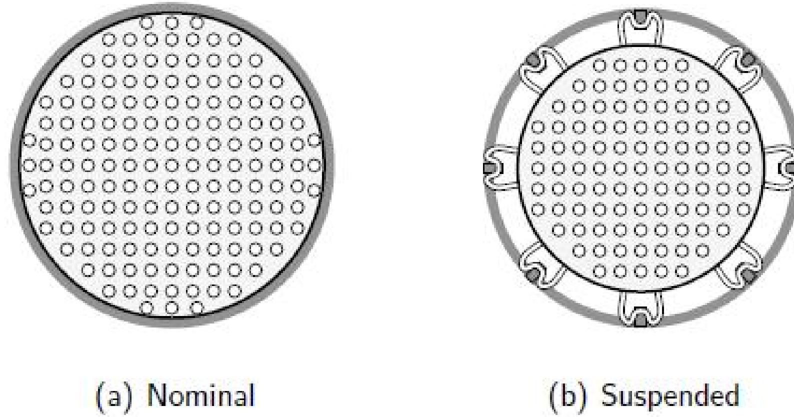

Figure 2.9: Comparison of backplate designs for freq. matching

In the nominal microphone design the resonance frequency of the backplate is higher than the membrane resonance frequency. In a new design to achieve frequency matching the backplate is suspended by micromachined springs instead of the common rigid connection. Fig.2.9 shows the comparison between the nominal, first-generation and the suspended designs. The stress in the backplate layer is reduced by the use of springs, thus making it more flexible, resulting in lower resonance frequency.

2.4 Compliance

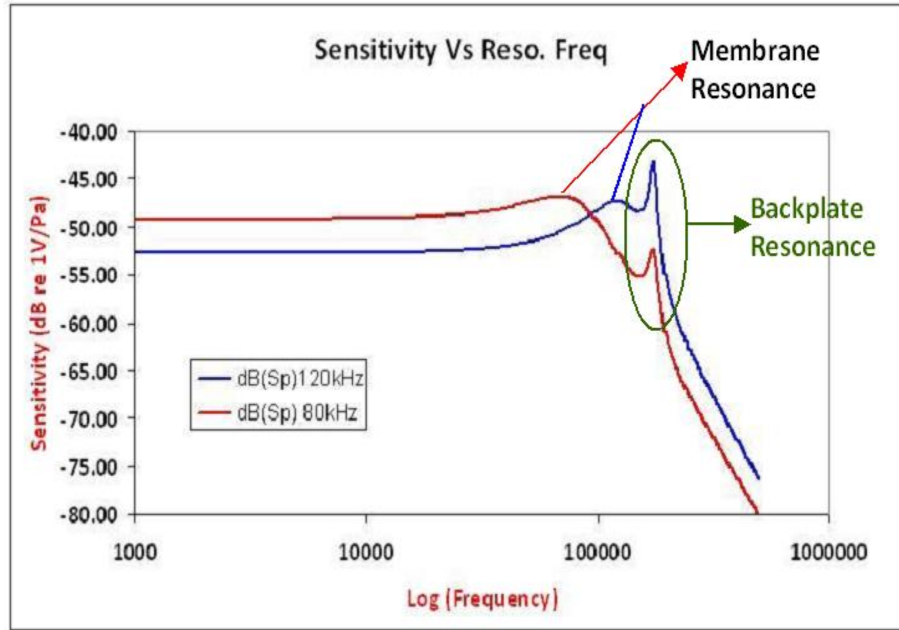

Figure 2.10: Frequency spectrum of the microphone with both membrane and backplate resonance frequencies, indicating that sensitivity increases with reduction in resonance frequency

As stated earlier, the elastic behavior of membranes is quantified by the term called compliance (Eqn.2.1) instead of the spring constant. Hence, we can express the resonance frequency as

$$f_{res} = \frac{1}{2\pi}\sqrt{\frac{1}{C * M}} \tag{2.10}$$

This expression shows the relation between the resonance frequency and the compliance. By reducing the resonance frequency, the compliance increases, leading to increase in sensitivity to acceleration. An increased sensitivity to acceleration implies that the membrane is more flexible, and thus also allows an increased acoustical sensitivity.

Fig.2.10 shows the frequency spectrum of the microphone obtained based on an approximate lumped element model. Both the membrane and backplate resonance frequencies are visible in the spectrum. Fig.2.10, shows that the acoustical sensitivity increases with reduction in membrane resonance frequency from 120 kHz to 80 kHz. In the lumped element model only the resonance frequency of the membrane is tuned and the backplate resonance frequency is not altered.

Chapter 3

Laser Vibrometer Measurement

This chapter focuses on the laser vibrometer measurement technique and the set-up used. Additionally, the results of the measurements are discussed.

3.1 Measurement Setup

Laser vibrometer measurement allows us to visualize the fundamental as well as the higher mode frequencies. Furthermore, it allows us to determine the displacement of the backplate due to an applied bias voltage. The operating principle of this setup is shown in Fig.3.1.

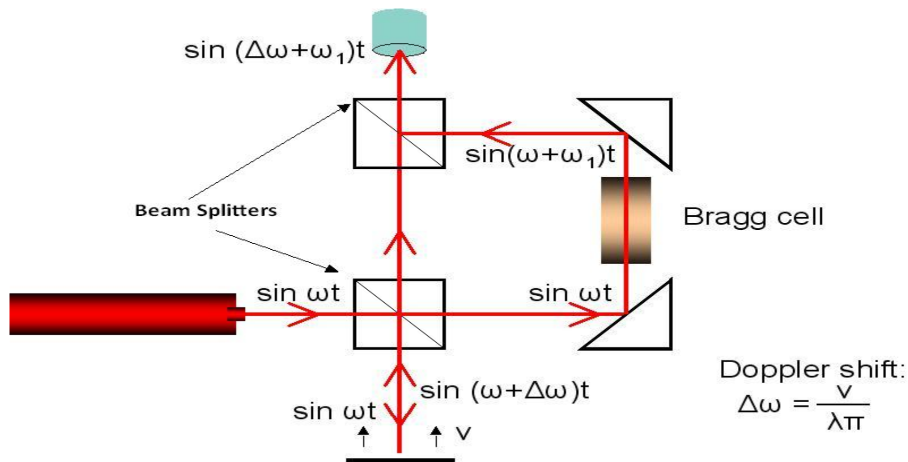

Figure 3.1: Polytec Laser Vibrometer working principle[13]

The laser beam is directed at the surface of the device, which is placed on the chuck, and the vibration amplitude and frequency are extracted from the Doppler shift of the laser beam frequency due to the motion of the surface. The beam from the laser is divided into a reference beam and a test beam

with a beamsplitter. The test beam then passes through the Bragg cell, which modulates the frequency. This beam is then directed to the target. The motion of the target adds a Doppler shift to the beam. The captured image is processed in the computer using the built-in algorithms. The result is visualized in the computer screen by the Polytec Laser Vibrometer software. The graphical user interface (GUI) of this software is shown in Fig.3.2, showing the movement of the backplate in the top half and the respective frequency spectrum with all the resonance peaks in the bottom half.

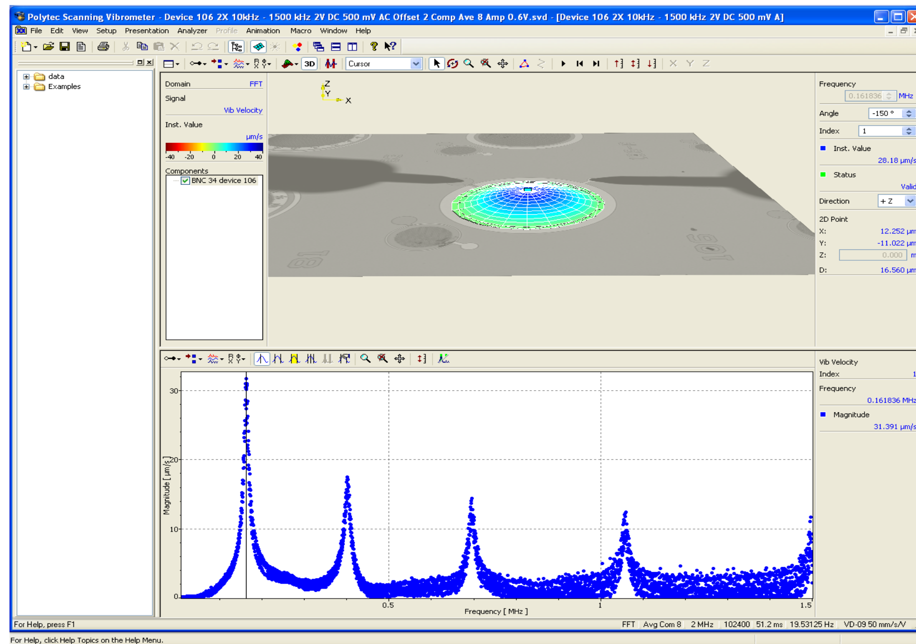

Figure 3.2: Polytec software interface and the measured resonance peaks of the backplate

We used this equipment to measure the resonance frequencies of the circular membrane and backplate. We note that we can only determine the different resonance peaks, (i.e) the fundamental resonance frequency and the higher mode frequencies, if the entire surface of the plate can be scanned with the laser.

In the case of the NXP MEMS microphone sensor, the membrane is located beneath the backplate, as was illustrated in Fig.2.3. Hence it is difficult to scan the surface of the membrane, while it is easy to investigate the backplate. We will, therefore, first discuss measurements on the backplate. At the end of this section we will show how the membrane can be investigated.

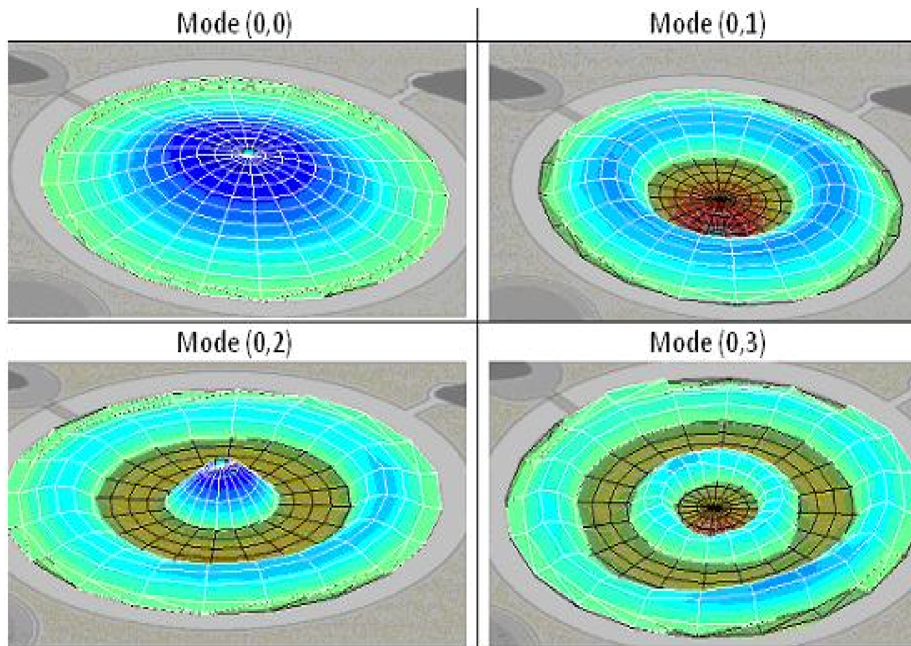

Figure 3.3: Measured fundamental and higher-order resonance modes of the backplate

Several higher modes of the circular backplate are shown in Fig.3.3. We performed this measurement in the laser vibrometer by selecting a specific scanning grid. This scanning grid consists of an array of measurement points on which the laser beam is consecutively focused during the measurement. Fig.3.4 shows the scanning grid formed over the backplate.

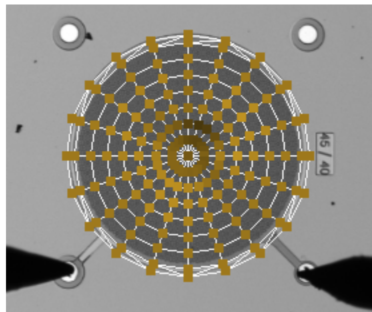

Figure 3.4: Scanning grid with scan points superposed on an optical image of the backplate

Two types of measurements are possible, a non-contact vibration measurement and a measurement that involves electrical actuation of the device. We will only discuss measurements on electrically actuated devices.

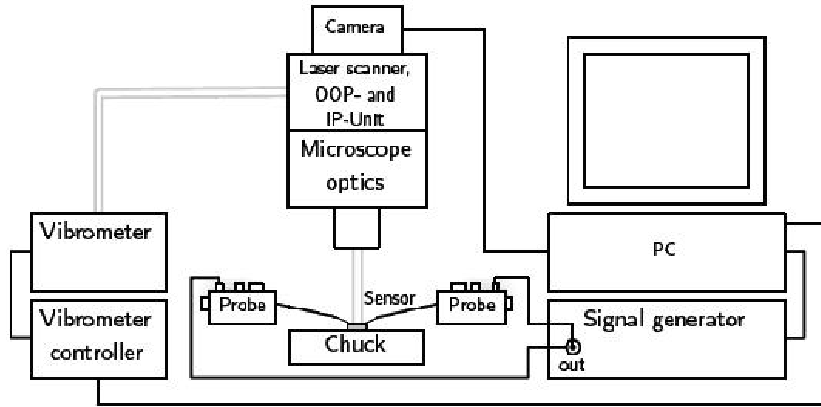

Figure 3.5: Polytec Laser Vibrometer Setup[10]

The Polytec laser vibrometer setup is shown in Fig.3.5. This setup is used for the electrical measurement in which the device is placed on the chuck and the probes are connected to the contacts. A constant DC voltage is applied with an actuation AC voltage from the signal generator to the microphone. The frequency is swept over a wide range from 1 kHz to 3.5 MHz. The frequency range limitations are based on the selection of specific vibrometer controller. This vibrometer controller allows us to select the correct decoder for the measurements. We can select the Vibrometer controller as either VD-06 (350 kHz) or VD-09 (2 MHz) based on the frequency range we need to measure. This laser vibrometer has a maximum frequency range of about 20 MHz and the resolution is down to tens of pico meters.

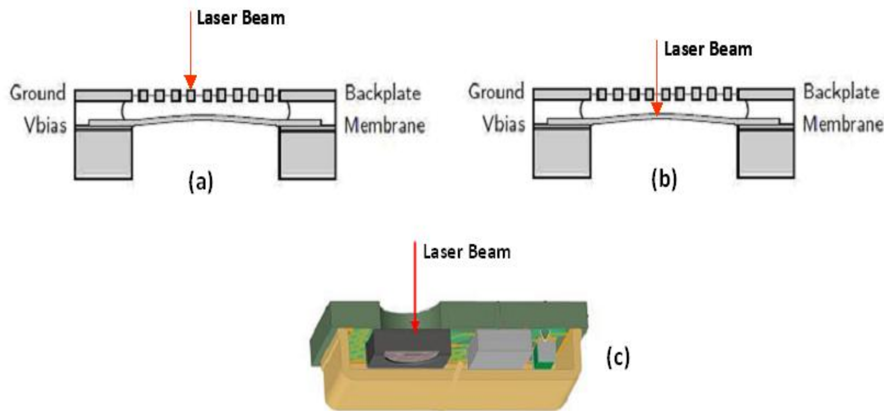

Figure 3.6: Different measurements performed on the laser vibrometer, (a) focusing laser beam on the backplate, (b) focusing laser beam on the membrane, (c) focusing laser beam through the acoustic hole on the membrane in a packaged sample

The observation of membrane movement from the bottom of the wafer is not possible with the current setup, since the laser beam as well as the electrical connections are made from the top. Fig.3.6 illustrates how we can perform measurements on the membrane, even though this is located below the backplate. As shown in Fig.3.6(b) the laser beam must then be focused through the backplate hole on the membrane. It is in this case not possible to scan the entire surface of the membrane. Fig.3.6(c) illustrates another membrane measurements. A packaged sample can be positioned such that the membrane is on top, so that we do not have to focus through the backplate hole. Commonly, we use a microscope objective with 2X magnification. In order to analyse the movement of the backplate and the membrane more in detail, we also use 50X magnification. We present the results in the next sections.

3.2 Test Measurements

Laser vibrometer measurements provide us with details about the operation of the device. Especially the deflection profiles can be measured and the resonances can be identified. Before presenting the actual measurement results in Sec.3.3, we will now discuss some test measurements.

The measurements are repeated several times to check the reproducibility of the measurement. These repeated measurements are done for the same conditions, (1) by repeating the experiment for several times without lifting the probe needles and (2) by lifting and re-connecting the needles after a single measurement. The repeated measurements revealed that the results do not change with repetition.

Furthermore, we performed a measurement to check the influence of vibrometer range of the Polytec setup on the measured readings. This is analyzed by performing a measurement for changing the vibrometer range for same conditions. The results for the varying vibrometer range prove that the choice of range does not influence the measured results.

The measurement plots supporting these conclusions are presented in Appendix B.

3.2.1 2X and 50X Magnification Measurement

We compared results for different magnification by performing measurements on the backplate of the device in wafer. We varied the AC voltages at different DC voltages for both 2X and 50X magnification. The advantage of 50X measurement is that we can focus the laser beam on the backplate perfectly and the real movement of the backplate can be analyzed.

The advantage of 2X magnification is that we have access to the entire backplate surface, allowing us to specify a grid (see Fig.3.4) and investigate the different resonance modes. Fig.3.7 shows the frequency spectrum of the device at 2X magnification. The backplate displacement is shown on the y-axis and it can be observed that the displacement peaks at resonance frequency (180 kHz). The displacements values plotted in Fig.3.8 are obtained at 40 kHz.

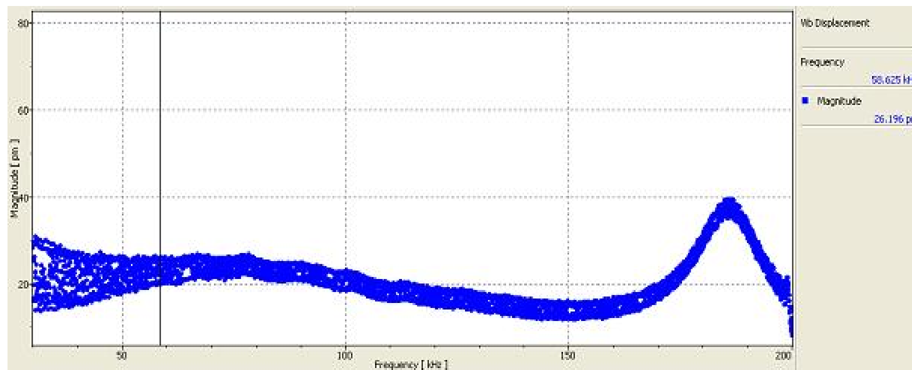

Figure 3.7: Backplate displacement at 2X normal magnification at 5Vdc and 0.3 Vac (Measurement)

Fig.3.8 shows that the displacement increases with the AC as well as the DC voltage.

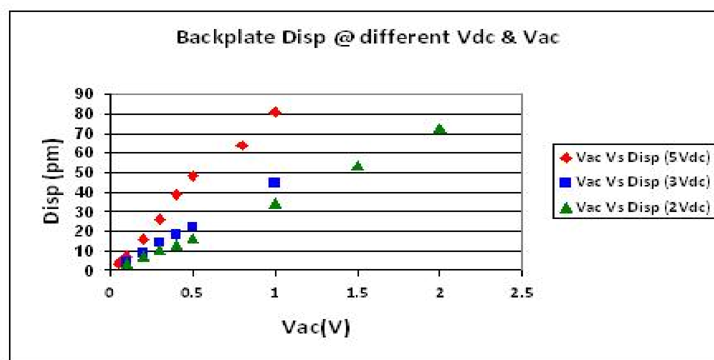

Figure 3.8: Backplate displacement at 2X normal magnification with respect to different DC and AC voltages (Measurement)

Fig.3.9 shows the frequency spectrum of the device at 50X magnification along with the backplate displacement in y-axis. Fig.3.10 shows the relation between the backplate displacement measured at 40 kHz with DC and AC voltages at 50X.

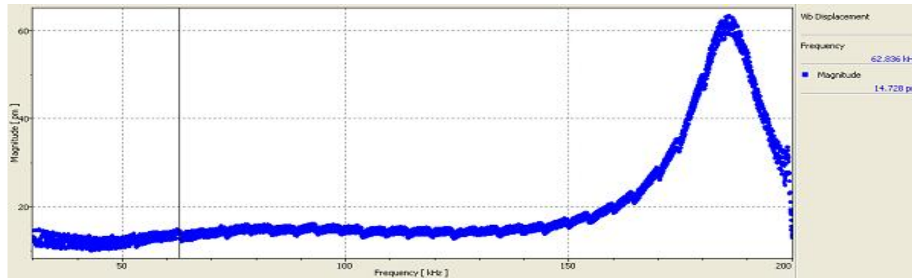

Figure 3.9: Backplate displacement at 50X magnification at 5Vdc and 0.5 Vac (Measurement)

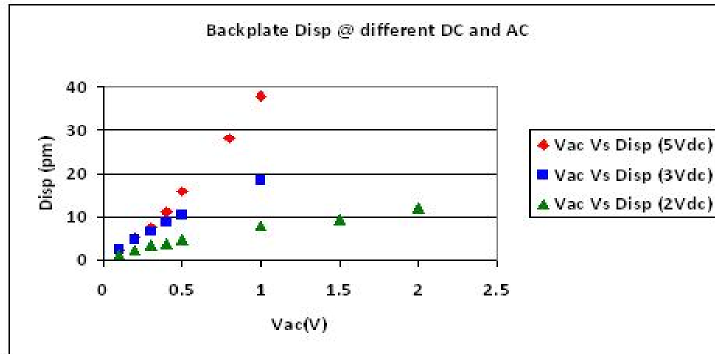

Figure 3.10: Backplate displacement at 50X magnification with respect to different DC and AC voltages (Measurement)

The 2X and 50X measurement results of the backplate show that the displacement increases for increasing AC and DC voltages. We note that the 2X magnification measurement is influenced by both membrane and backplate movement, because the laser beam can scatter at the backplate holes or it might even pass through the holes. The 50X magnification measurement, on the other hand, only measures the backplate deflection. Since it allows us to focus the laser beam on the region between the holes, it gives the pure displacement of the backplate. This gives us an idea that the reading obtained from 50X offers the real backplate movement. However, the 50X magnification does not allow to scan the displacement profile over the full backplate. The 2X magnification should therefore be used to measure qualitative mode shapes. The measured mode-shapes agree well with the expectations that the next higher order has one nodal line (zero amplitude) more than the previous.

3.3 Backplate Frequency Measurement Results

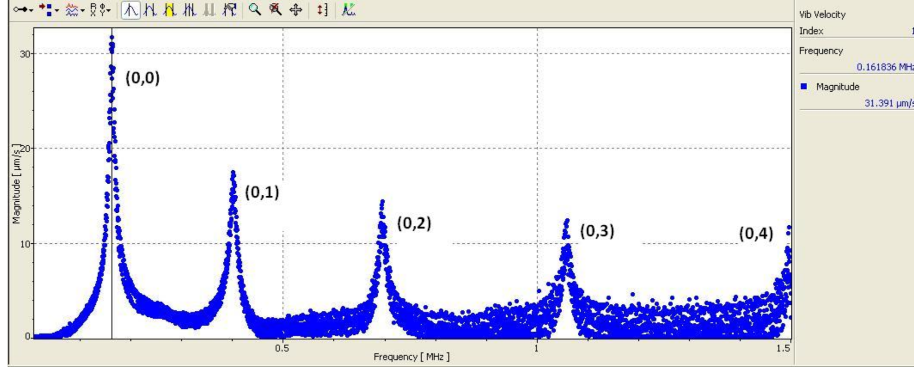

Figure 3.11: Frequency spectrum of backplate measured in laser vibrometer. Also higher mode frequencies are visible

This measurement is performed on the wafer sample shown in Fig.2.4. The wafer is placed on the chuck below the laser scanning head of the measurement setup. The backplate is on top and can thus be easily scanned. The backplate resonance frequencies are measured at the normal 2X magnification. We actuated the backplate by applying an AC voltage of 50mV. Due to the electrostatic force between the backplate and the membrane, the plates will oscillate at the applied frequency. In addition, we applied a DC voltage and performed measurements for V_{DC}= 5V. The different resonance modes observed from the backplate are shown in Fig.3.3 and the corresponding frequency spectrum is shown in Fig.3.11. Table.3.1 shows the comparison between measured and calculated backplate resonance frequencies. The higher-order resonance frequencies are calculated using the Eqn.4.11. First from the measured f(0,0) frequency, the stress value is calculated using the Eqn.4.11 and by using the stress value and corresponding Eigen values, the higher-order frequencies are calculated.

Backplate Resonance Modes	**Measured (kHz)**	**Calculated (kHz)**
f(0,0)	162	162 (Measured)
f(0,1)	402	368
f(0,2)	695	577
f(0,3)	1060	787

Table 3.1: Comparison of measured and calculated higher mode frequencies

It is observed that the calculated values for the higher modes are different from the measured frequencies (see Table.3.1). The reason for this difference is the bending stiffness of the backplate. The bending stiffness of the tension dominated backplate is related to the stress and thickness. Here the equation (Eqn.4.11) used to calculate the higher modes are based only on the stress, and the thickness is neglected. This thickness term and additionally the material properties like Young's modulus will have some influence on the resonance

frequency which leads to the difference between the calculated and measured values.

Both stress and resonance frequencies are related to each other through the Eqn.4.11. It is to be noted that the initial stress in the backplate is 160MPa after deposition, while the stress calculated using the measured resonance frequency is 64MPa. If we use 160MPa for calculating the first resonance frequency using the Eqn.4.11 we end up with 215 kHz, while in reality the measured frequency is 162 kHz. Finite element method (FEM) simulations show that the initial stress of the backplate layer relaxes to 65 MPa as the plate is patterned [7]. This indicates that the measurement results are in good agreement with the simulations.

3.4 Measurement of membrane at Low Frequency

3.4.1 Wafer sample measurement

We investigated the membrane as was illustrated in Fig.3.6(b). This measurement is performed to analyze the frequency response below the membrane resonance frequency. These measurements are performed on the microphone samples on the wafer, without package.

In order to analyze the displacement, different measurements are performed such as varying the AC voltage at different DC voltages. These measurements are performed at higher magnification 50X in order to focus the laser beam through the backplate hole on the membrane. Fig.3.6(b) shows this measurement set-up.

Fig.3.12 shows the frequency spectrum of the device along with the membrane displacement in y-axis. The measured results show that the displacement values are high when compared to backplate displacement (see Fig.3.10), since the membrane is more flexible. Fig.3.13 shows the dependence of the membrane displacement on DC and AC voltages. The membrane displacement increases as expected. We note that this measurement is complicated as it is hard to focus the laser beam through the holes. The results are therefore not so accurate.

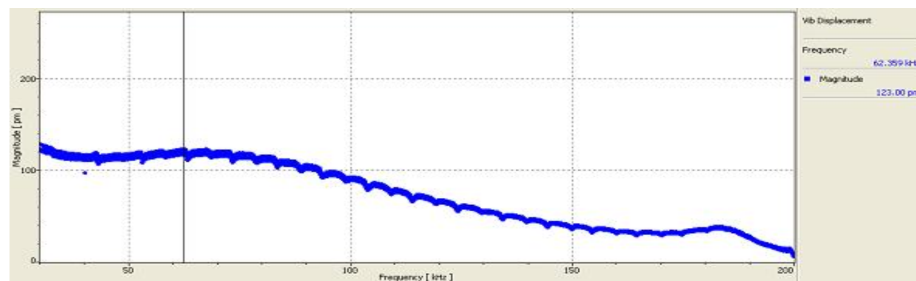

Figure 3.12: Membrane displacement seen through the backplate holes at 5Vdc and 0.5 Vac (Measurement)

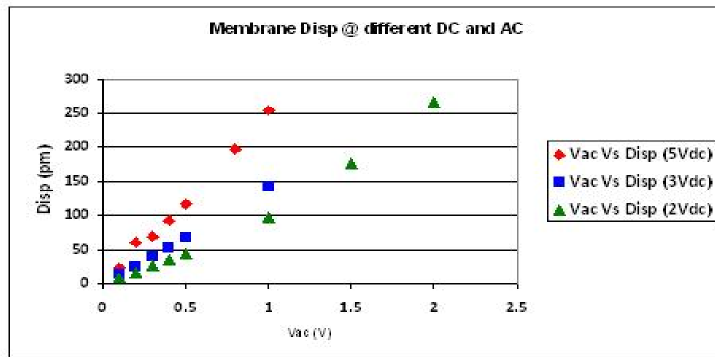

Figure 3.13: Membrane displacement with respect to different DC and AC voltages (Measurement)

3.4.2 Packaged sample measurement

This measurement is performed to scan the membrane surface to identify the influence of the package on the resonance modes of the membrane. The packaged sample is used in the laser vibrometer measurement as shown in Fig.3.6(c). In this measurement the laser beam is focused on the membrane through the acoustic hole.

The acoustic hole is not placed above the center of the membrane and it only allows optical access to a section of the membrane. The frequency spectra of the measured device for two different frequency ranges are shown in Fig.3.14 and Fig.3.15.

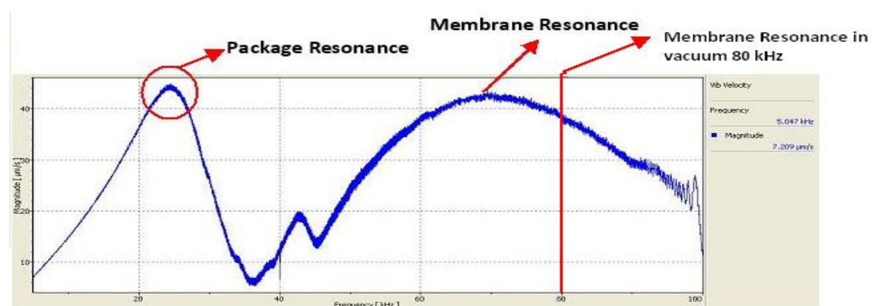

Figure 3.14: Measurement of membrane frequency spectrum of a packaged sample till 100 kHz in laser vibrometer (Measurement)

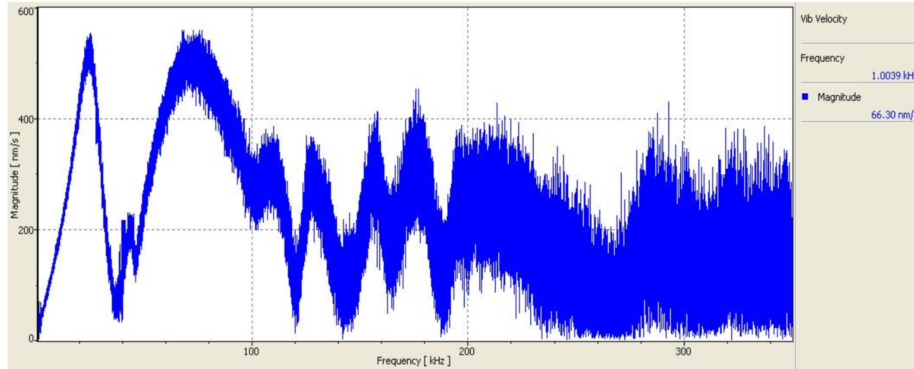

Figure 3.15: Membrane frequency spectrum of a packaged sample till 350 kHz (Measurement)

Fig.3.14 clearly shows the presence of an extra resonance at approximately 25 kHz, which is as strong as the membrane resonance. We attribute this extra resonance to the package. In Fig.3.15 it is impossible to identify the resonance frequency of backplate because of the interference with resonances caused by the air enclosed in the package.

3.5 Extraction of Electrostatic Force

The low frequency measurements are performed to find a way to extract the electrostatic force acting on the membrane and backplate. A simple electrostatic force equation used from displacement (x) and spring constant (k) the electrostatic force (F_e) can be written as (Hookes Law),

$$x = \frac{F_e}{k} \tag{3.1}$$

the spring constant in this equation can be used either from the membrane or backplate to extract the force acting on them. The displacement obtained for the backplate at 50X magnification at 5V and 1 Vac is around 38pm (see Fig.3.10) and the spring constant calculated for the backplate using Eqn.3.2 is 2406 N/m.

$$C_m = \frac{1}{2\rho h \pi^3 R_m^2 f_{res}^2(0)} \tag{3.2}$$

Finally the AC electrostatic force extracted using Eqn.3.1 is 91nN. This is a rough and very simple calculation, it gives an idea of the amount of electrostatic force acting on the backplate and we did not derive a theoretical expression to compare this value.

3.6 Summary

In this chapter, we first discussed about the laser vibrometer operating principle and its measurement setup. Then the test measurements performed such as, repeatability measurement, changing vibrometer range measurement and 2X

and 50X magnification measurement were shown. Later the measurements on backplate and membrane in both the wafer and package sample were discussed and finally an introduction about electrostatic force extraction was shown.

From the backplate frequency measurement, both the theoretical and measured frequencies are compared and the difference between the values is analyzed. It is identified that the difference is due to the bending stiffness of the backplate and stress relaxation due to backplate perforation. The stress values extracted from the measured frequencies are in good agreement with the FEM simulations.

The low frequency measurements are performed to analyze the displacement of backplate and membrane. These measurements are performed at both 2X and 50X magnifications. From the results, the trend of the displacement with respect to AC and DC voltages are identified. We note that the results from 2X measurements are not accurate because the laser beam can scatter through the backplate holes or it can pass through the holes at certain scanning region of the backplate. This disadvantage is avoided in 50X magnification measurement since it focuses only on the no hole region of the backplate very accurately and it gives the pure displacement of the backplate. However, the 50X magnification does not allow to scan the displacement profile over the full backplate. The 2X magnification should therefore be used to measure qualitative mode shapes.

A 50X measurement is performed to analyze the displacement of membrane. This measurement is complicated as it is hard to focus the laser beam through the holes and the results are not so accurate because of scattering caused by the edge of holes or the moving membrane. This displacement measurement is used to extract the electrostatic force measurement using the Hookes law. The simple calculations provided the amount of force acting on the backplate.

Finally the packaged sample measurements provided an overview of the air damping inside the package. This results in shifting the resonance frequency of the membrane. This packaged measurement results (Fig.3.15) looks similar to the results (Fig.4.11(c)) obtained from electrical impedance measurement of packaged sample under air.

Chapter 4

Electrical Impedance Measurement

This chapter focuses on the electrical impedance measurement. We used two setups for this experiment. Also the extraction of key parameters such as resonance frequency and compliance along with the results obtained are discussed.

4.1 Frequency Response Measurement

As stated earlier in Chapter 2 the measurement of the device frequency response is necessary to analyze the device performance. Here the same frequency response is measured and the mechanical resonances of membrane and backplate show up in the electrical impedance of the sensor.

Impedance is the hindrance to the flow of alternating current . Impedance (Z) is expressed as a combination of Resistance (R) and Reactance (X) and is measured in ohms (Ω) [14]. It can be expressed as a complex quantity:

$$\mathrm{Z} = \mathrm{R} + \mathrm{j}\ \mathrm{X}$$

This impedance measurement offers access to the dissipation. Dissipation is also denoted as losses and this can be calculated from the measured real and imaginary part of the impedance (Eqn.4.1). This dissipation will be high at resonance frequency f_{res} and it can be seen in Fig.4.1. This dissipation peaks at the resonance frequency because of the large change in capacitance at resonance and it dissipates more energy. This helps us to determine the resonance frequency of the membrane and backplate.

$$D = \frac{Re(Z)}{|Im(Z)|} = \frac{R}{|X|} \tag{4.1}$$

Another electrical measurement is the Capacitance – Voltage (C-V) measurement. As the name states, this measurement is to determine the dependency of capacitance between the microphone membrane and backplate with respect to the DC voltage. It helps to determine the mechanical compliance of the membrane (C_m).

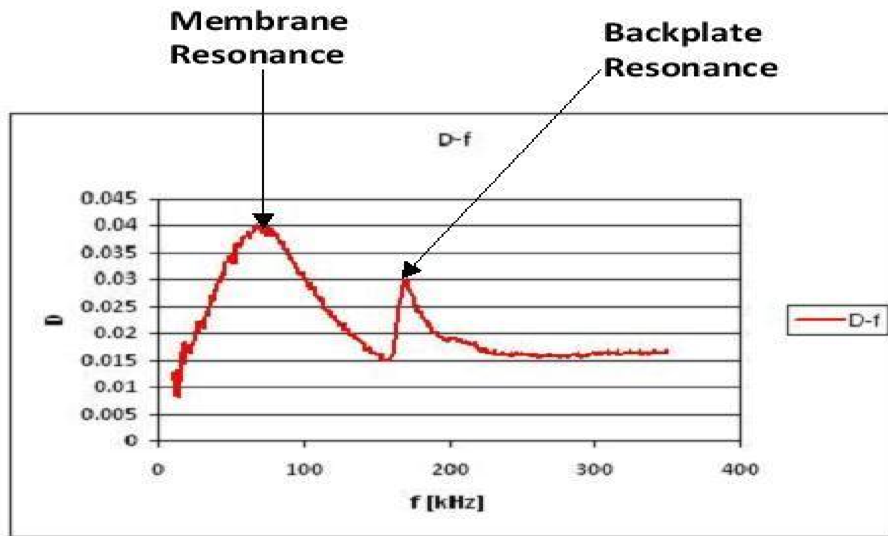

Figure 4.1: Dissipation as a function of frequency (Measured)

4.1.1 Measurement Set-ups

The measurement set-up used is a HP Impedance Analyzer (HP 4194A) probe station. Fig.4.2 shows the experimental set-up for the measurement. The figure shows the set-up in vacuum conditions, the same set-up can be used for the air measurements without the vacuum chamber. The advantage of vacuum measurement is that clear and sharp peaks can be seen at resonance whereas the air damping shifts and broadens the resonance peaks.

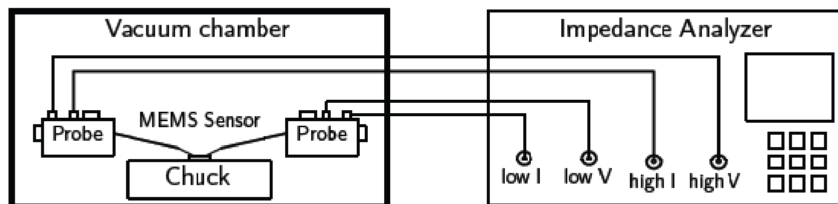

Figure 4.2: Electrical Impedance measurement setup

The MEMS microphone is placed on the chuck and the probe needles are connected to the membrane and backplate contacts. The high potential is connected to the membrane and the low one is connected to the backplate contact. Since this is an electrical measurement we need to apply an external potential to actuate the device. This setup can be used for both frequency-dependent and voltage-dependent measurements.

Other setup used is the HP Multifrequency RLC – meter (HP 4275A). Fig.4.3 shows the measurement setup used for this impedance measurement. It is mostly used for capacitance voltage measurement. MEMS microphone is placed on the

chuck and the probes are connected same as for the Impedance measurement.

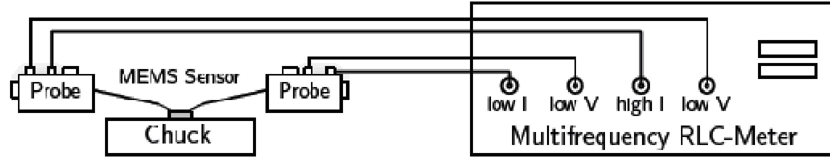

Figure 4.3: Capacitance - Voltage measurement setup

4.1.2 Measurement setup Calibration

Both these measurement setups are calibrated in a different way. The HP impedance analyzer is calibrated using an external standard substrate, which consists of different resistors of standard (50Ω) values and short circuit connections.

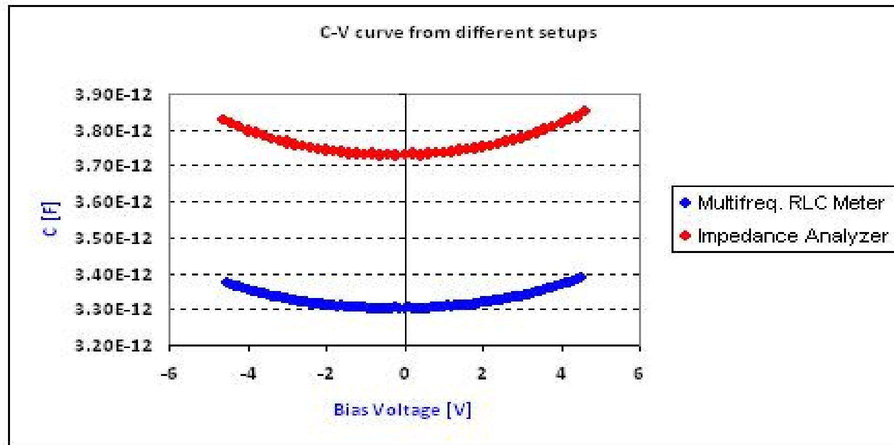

Figure 4.4: Comparison of measurement setups C-V curve measured (Before)

Those standard and short circuit connections are used to calibrate the impedance analyzer together with an open circuit calibration. On the other hand just an open calibration is performed for the RLC Multifrequency meter by just pressing a button in the setup.

We performed tests to check whether the measurement setups provide similar results. Capacitance voltage measurement is performed on HP Impedance analyzer and HP RLC Multifrequency meter for five MEMS microphone samples under same conditions. It is observed that the capacitance voltage curves measured for five samples using the two setups with same measurement conditions are different. It shouldn't be the case, since the samples have to give the same capacitance values for both setups. This difference can be seen in the capacitance voltage curve in Fig.4.4 and it shows the comparison of C-V curve for one sample between two setups.

In order to analyse the difference between the setups a fixed capacitance measurement is performed on both setups. The fixed capacitor is a ceramic capacitor with a value of 3.9 ± 0.1 pF, whose value is stable over a wide range of voltage and frequency. After measuring the capacitor in both setups for a variety of frequency and voltages, the result obtained from HP Impedance analyzer is 4.46pF and from the RLC Multifrequency meter is 3.87pF. This gives us an idea that there is a difference of around 0.5pF measured from the Impedance analyzer and it caused the difference in measured capacitance results.

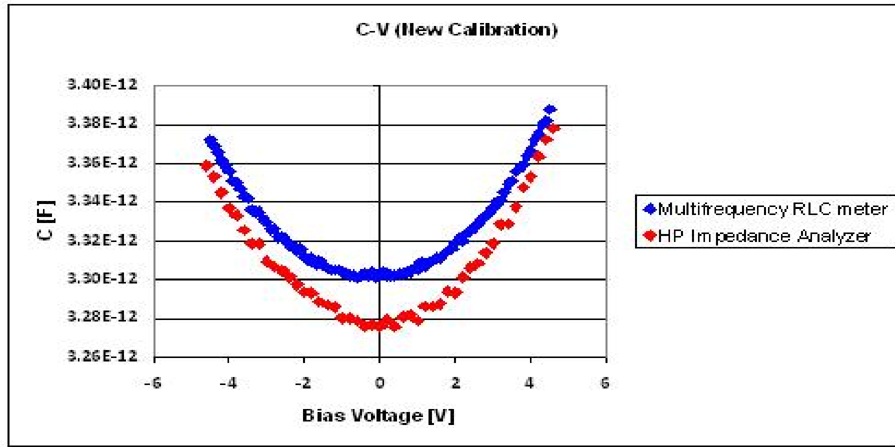

Figure 4.5: Comparison of measurement setups C-V curve measured(After)

We found that the differences between both setups are because of the calibration techniques used. The cause for the problem is identified as the 50Ω resistors in the external standard substrate. Since the device is old and the repeated use before every measurement caused the device to degrade and it is no more equal to 50Ω (Standard value) but was between 53Ω and 60Ω. Using the degraded device to calibrate the impedance analyzer caused difference in the measurements. Finally the open calibration method used in the RLC Multifrequency meter is followed in the HP Impedance analyzer. Since this is the most robust calibration for the low frequency and small capacitances which gives the least calibration uncertainties. After this change in calibration method, capacitance values measured agrees each other quite well in both setups. Fig.4.5 shows the C-V curve with new calibration technique.

From Fig.4.5 we can see that the difference between the two setups measured capacitance voltage curves are now reduced from 0.5pF to around 0.02pF. This difference is reasonable and it could be from the parasitic capacitances of the probes to the microphone substrate. The influence of calibration techniques on the membrane compliance extracted are listed in Appendix A.

4.2 Resonance Frequency

First we will show how the pure mechanical resonance frequency is extracted from the electrical impedance measurement. Pure mechanical resonance frequency is the value obtained at zero bias voltage. At zero bias voltage the

resonance is not visible in the electrical signal, but the 0V frequency can be extrapolated.

In general the mechanical resonance frequency of the spring mass system is given by the equation [11]

$$f_{res} = \frac{1}{2\pi}\sqrt{\frac{K_{eff}}{m_{eff}}} \tag{4.2}$$

where K_{eff} is the effective spring constant in N/m and m_{eff} is the effective mass in kg, ρ is the density of silicon in kg/m^3, h_m is the thickness of membrane in m and R_m is the radius of the membrane in m. Effective parameters are used here because the membrane is not rigid and therefore cannot be regarded as a point-mass. Assuming a parabolic deflection profile, the effective membrane mass equals half the actual mass [11].

$$m_{eff} = \frac{m}{2} = \frac{1}{2}\rho h_m \pi R_m^2 \tag{4.3}$$

In order to use this Eqn.4.2 for our resonance frequency measurement, a slight modification has to be done. In our case K_{eff} is a combination of both mechanical and electrical spring constant in which the mechanical part (K_m) is independent of the bias voltage and the electrical part (K_{el}) is completely dependent on the bias voltage. This can be given by the equation

$$f_{res}(V_{bias}) = \frac{1}{2\pi}\sqrt{\frac{K_m - K_{el}(V_{bias})}{m_{eff}}} \tag{4.4}$$

Here the electrical spring constant takes the negative sign, since it acts against the mechanical spring force. The electrical spring constant for center deflection is given by the equation [11]

$$K_{el}(V_{bias}) = \frac{\varepsilon \pi R_m^2 V_{bias}^2}{2g^3} \tag{4.5}$$

where ε is the dielectric permittivity of air, R_m is the radius of the circular membrane or backplate and g is the air gap between the membrane and backplate. Replacing K_{el} in Eqn.4.4 [11]

$$f_{res}(V_{bias}) = \frac{1}{2\pi}\sqrt{\frac{K_m}{m_{eff}} - \frac{\varepsilon \pi R_m^2 V_{bias}^2}{2g^3 m_{eff}}} \tag{4.6}$$

From this equation it is clear that the resonance frequency depends on the bias voltage. With increase in the bias voltage the resonance frequency shifts down. This effect is called the Electrostatic Spring Softening. We need to correct for this effect in order to determine the pure mechanical resonance frequency.

Additionally the higher harmonics and the resonances of the backplate can be measured. This can be useful to compare and validate with finite element simulations [7].

4.2.1 Extraction of Resonance frequency

As stated earlier this measurement is performed in the HP Impedance analyzer and this is done in both air and vacuum conditions. This measurement is performed to measure the complex impedance and the main task is to identify the mechanical resonances of both membrane and backplate. This measurement is done at different bias voltages V_{bias} superimposed with an actuation voltage V_{ac} and by sweeping the frequency over a wide range. This AC voltage acts as an actuation voltage for the oscillating membrane.

The complex impedance is represented by series capacitance C_s and dissipation factor D. Alternatively, parallel capacitance C_p can be selected but the problem with this C_p is that the value drops at higher frequencies due to the series resistance of the electrodes. This drop can be seen during the measurements that the value of series capacitor at 2 MHz is 3.3 pF and the parallel capacitor is 2.9 pF (Fig.4.6).

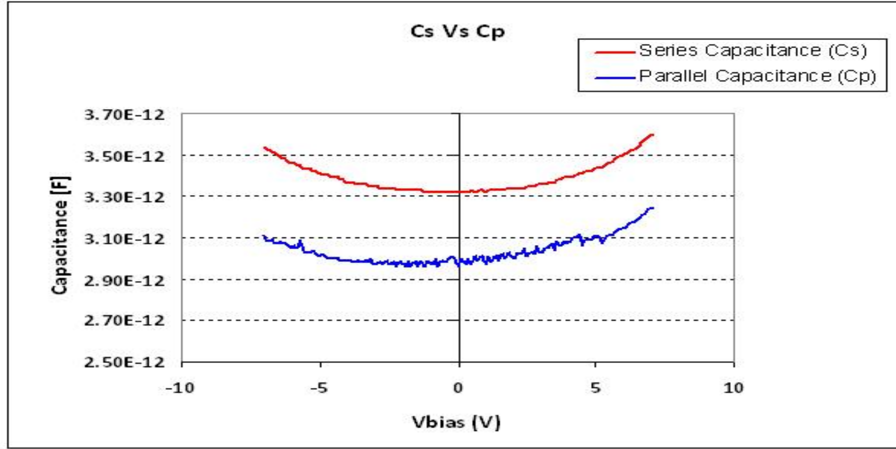

Figure 4.6: Series capacitance Vs parallel capacitance at 2MHz (Measured)

The dissipation (D) is calculated using the Eqn.4.1 and it is plotted as a function of frequency. Fig.4.7(a) shows the dissipation (D) as a function of frequency in air. It can be seen that there are two peaks indicating the fundamental resonance of membrane around 75 kHz and the fundamental resonance of backplate around 170 kHz. Since this measurement is performed in air the resonance peaks are strongly damped due to the friction with the air. The same dissipation as a function of frequency measured in vacuum can be seen in Fig.4.7(b). Here the peaks are sharp and its easy to identify the resonances. Additionally the peak seen at the 200 kHz in vacuum is the first higher mode of the membrane which will be discussed in the later section.

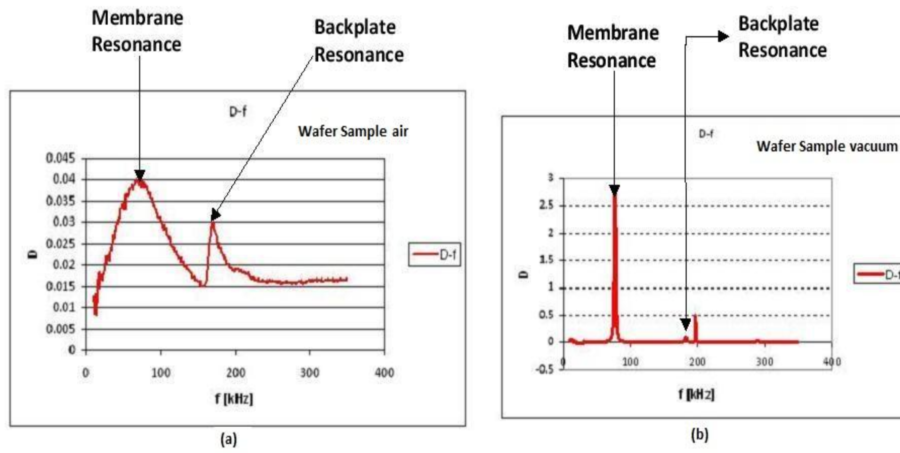

Figure 4.7: Dissipation as a function of Frequency as extracted from impedance measurement performed in (a) air (b) vacuum

Also the series capacitance is calculated from the measured impedance using the Eqn.4.7. This helps us to identify the resonance frequency since the capacitance drops at the resonance.

$$C_s = \frac{-1}{Im(z) * \omega} \tag{4.7}$$

$$\omega = 2\pi f \tag{4.8}$$

Fig.4.8 shows the series capacitance as a function of frequency in both air and vacuum. It is observed that the capacitance change at resonance in vacuum is sharp and the values are large indicating the resonance frequencies.

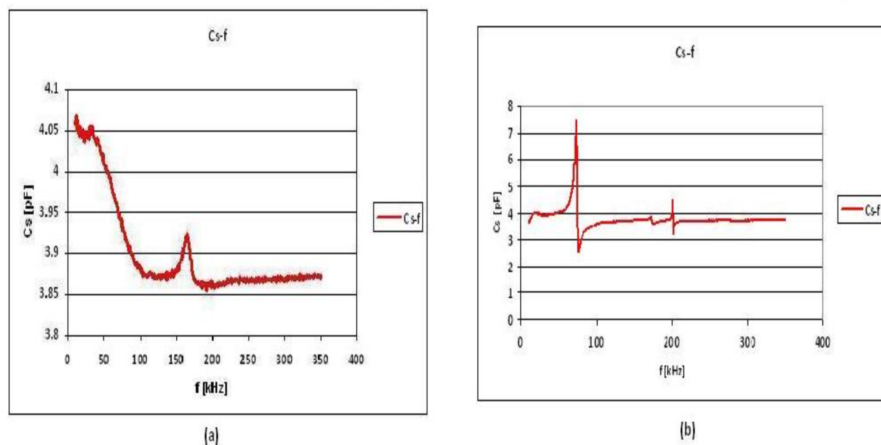

Figure 4.8: Series Capacitance as a function of Frequency as extracted from impedance measurement performed in (a) air (b) vacuum

As said earlier this resonance frequency includes the electrical part. From the Fig.4.9, we can see that the dissipation increases with increase in bias voltage indicating that the peaks are getting steeper and the frequency shifts down. This effect is used for extraction of the mechanical resonance frequency. In order to extract the mechanical resonance, the Eqn.4.6 can be rewritten as,

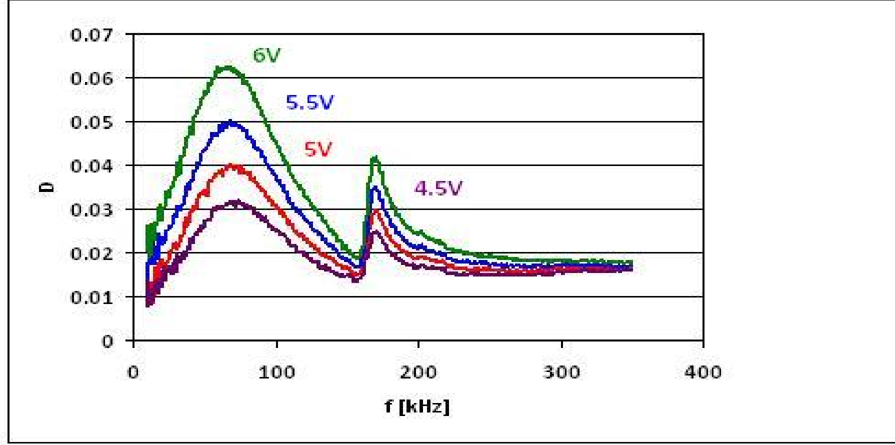

Figure 4.9: Dissipation as a function of frequency measured for several bias voltages

$$f_{res}(V_{bias})^2 = f_{res}(V_{bias} = 0)^2 - \frac{\varepsilon \pi R_m^2}{8\pi^2 g^3 m_{eff}} V_{bias}^2 \tag{4.9}$$

This shows that there is a linear relation between V_{bias}^2 and f_{res}^2. The frequency at which the dissipation is high is collected for each bias voltage and f_{res}^2 is plotted against V_{bias}^2 (Fig.4.10). Since this relation is linear we obtain a linear fit, which can be related to Eqn.4.9 to extract the mechanical resonance frequency at zero bias voltage.

The linear equation obtained from the plot is

$$f^2[kHz^2] = -64.2\left[\frac{kHz^2}{V^2}\right] + 6830\left[kHz^2\right]$$

Comparing with Eqn.4.9 at Vbias = 0V,

$$f_{res}^2(V_{bias} = 0) = \sqrt{6830kHz^2} = 83kHz$$

Mechanical resonance frequency obtained for the membrane is 83kHz and for the backplate is 170kHz in air for the wafer sample.

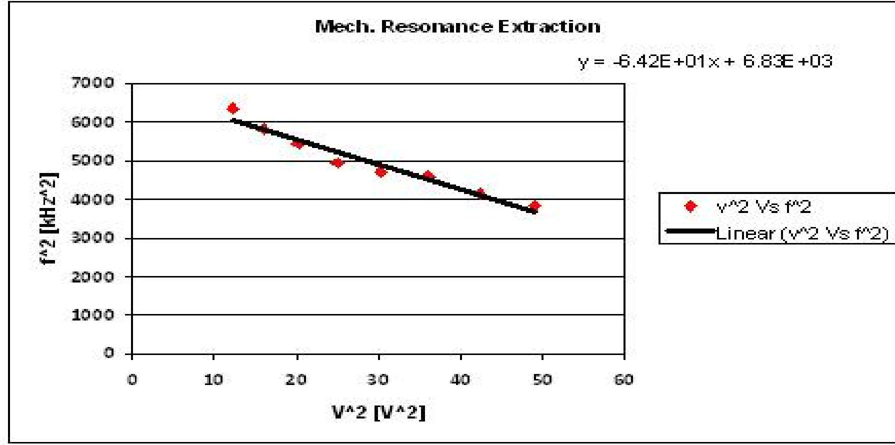

Figure 4.10: Linear plot of Frequency square Vs Voltage Square

The error associated with the resonance frequency can be calculated using the following procedure. A function called **LINEST (known_y's, known_x's, const, stats)** is available in the Microsoft Excel program, in which

- **known_y's** is the frequency square value
- **known_x's** is the voltage square value
- **const** is a logical value specifying whether to force the Y-axis crossing to equal 0. In our case we don't want to force our constant to zero. Thus it is selected as TRUE or 1.
- **stats** is a logical value specifying whether to return additional regression statistics. If this term is TRUE or 1, the function will return us the errors associated with the obtained values.

For example, the LINEST function result for the linear fit in Fig.4.10 is given in Table4.1 in which, $f_{res}(0)^2$ is the constant and $\sigma_{f^2_{res}(0)}$ is the error associated with the constant and the term $'-64.2[kHz^2] = -\frac{\varepsilon\pi R^2}{8\pi^2 g^3 m_{eff}}'$ which is related to the slope 'm' and the error associated with the slope is σ_m.

$\mathbf{m}[\frac{kHz^2}{V^2}]$	-64168933.12	$f_{res}(0)^2[kHz^2]$	6833429194
$\boldsymbol{\sigma}_m[\frac{kHz^2}{V^2}]$	5819521.533	$\sigma_{f^2_{res}(0)}[kHz^2]$	182159506.7

Table 4.1: LINEST function data of the linear fit

The error equation obtained for resonance frequency using error linearisation is given in Eqn.4.10 and the statistical error in the membrane resonance frequency is 1 kHz.

$$\sigma_{f_{res}}(0) = \frac{\sigma_{f^2_{res}(0)}}{2f_{res}(0)} \tag{4.10}$$

4.2.2 Air and Vacuum Measurement Results

As said earlier, this impedance measurement was measured under both air and vacuum conditions. The measurements are performed on both wafer (Fig.2.4)

and packaged samples (Fig.2.5). As was shown in Fig.4.7 it is easy to identify the sharp peaks of the resonance frequency of both membrane and the backplate. Additionally the higher mode frequencies are visible in the vacuum measurement, which can be compared with the laser vibrometer measurement. This air and vacuum measurement comparison is used to check the influence of the air damping and the back volume on the moving membrane. Damping is the effect that reduces the amplitude of the oscillation. In our case, the resonance peaks are damped which will shift the resonance frequency of the membrane. This effect can be seen clearly in the measurement results obtained.

4.2.2.1 Wafer and Packaged Sample Measurement Results

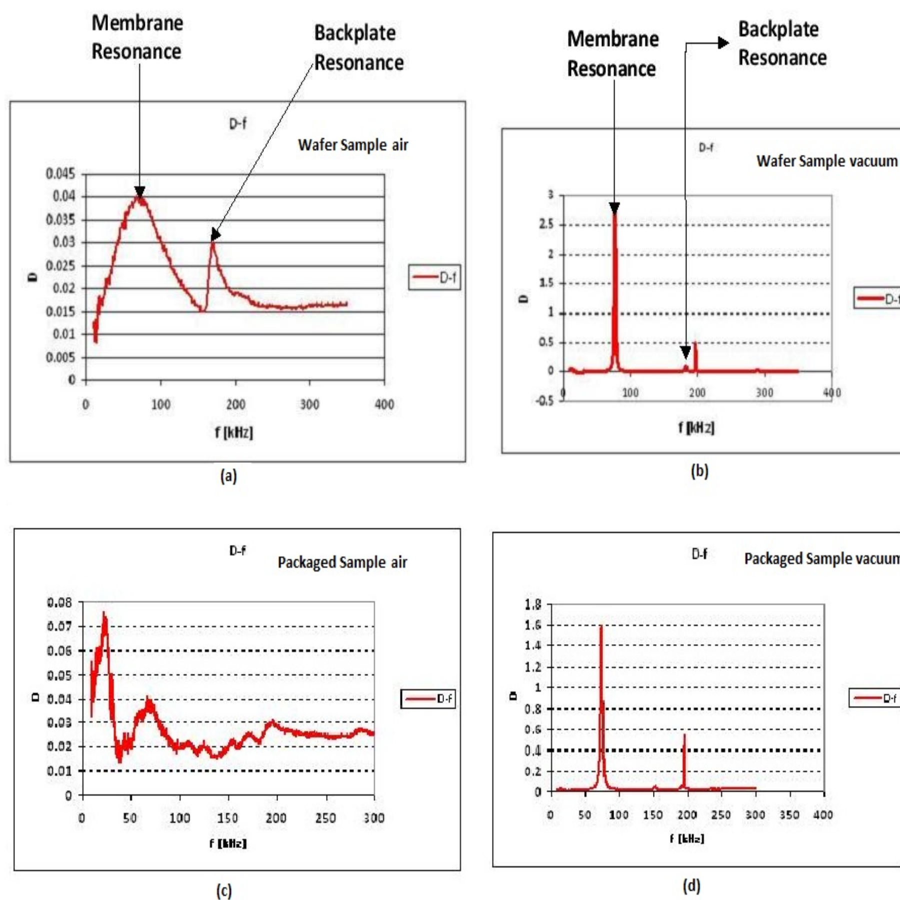

Figure 4.11: Comparison of Dissipation Vs Frequency for both wafer and packaged sample (Measurement)

First the impedance measurement results obtained from the wafer and packaged sample in both air and vacuum conditions are discussed. Fig.4.11 shows the dissipation vs. frequency plot obtained for both wafer and packaged sample in air and vacuum.

The difference between the two measurements can be clearly seen from the Fig.4.11(a) and (b). The air damping of the resonance frequencies are understood from the broad and sharp peaks. The mechanical resonance frequencies extracted from different samples both in air and vacuum conditions are listed in the Table.4.2.

From the values listed in the Table.4.2 it is observed that the membrane resonance frequencies extracted from the wafer samples in air are almost in the same range as that of vacuum. It shows that the air damping in case of wafer measurements are not affecting the resonance frequencies of the membrane much. The reason could be that the wafer is placed over the chuck and the back volume is nearly infinite and the air passage is very smooth without affecting the oscillating membrane much.

Wafer Sample No	**Resonance in air (kHz)**	**Resonance in vacuum (kHz)**		**Packaged Sample No**	**Resonance in air (kHz)**	**Resonance in vacuum (kHz)**
1	82 ± 0.8	84 ± 1.0		1	74 ± 1.0	83 ± 0.7
2	79 ± 0.8	80 ± 0.8		2	75 ± 0.9	81 ± 0.8
3	82 ± 0.4	84 ± 1.0				
4	81 ± 0.6	81 ± 0.9				
5	83 ± 1.0	82 ± 0.8				

Table 4.2: Membrane resonance frequencies in air and vacuum for both wafer and vacuum samples (Measurement)

On the other hand the results obtained for the package samples in both air and vacuum conditions are different. This can be observed in the Fig.4.11(c) that the influence of air in the package is quite high on the moving membrane. It is almost impossible to identify the backplate resonance frequency in air measurement. Additionally we see a peak at low frequency range at around 23 kHz. This peak is also visible in the Laser Vibrometer packaged sample measurement in Fig.3.14. This peak is assumed as the resonance of the package, where the air in the package is dominating the membrane resonance and it shifts its frequency.

If we compare the membrane frequency results extracted from both wafer and package samples in vacuum measurements they are almost matching with each other. This gives a good sign that the results obtained from vacuum measurements give info about the membrane instead of the package. The comparison between Fig.4.11(c) and (d) gives an idea what's the effect of damping on the moving membrane. It seems to be quite high. Hence an optimal back volume that is the volume inside the package has to be selected which gives a good sensitivity for the present device parameters such as 5V bias, 2 µm air gap, area of membrane and effective compliance. The back volume selected for the device is $4mm^3$, the reason to select this back volume is that, increasing the back volume for increased sensitivity could shift the first package resonance into the audio range and more obvious reason is that the customer will not be interested in big size packaged device.

4.2.2.2 Backplate resonance frequency and stress

The resonance frequency of the backplate can be extracted in both cases in the same way as explained for the membrane in Sec.4.2.1 and the values obtained are around 180 kHz these values are listed in Table.4.3.

The backplate resonance frequencies listed in Table.4.3 for both air and vacuum conditions are almost same. This indicates that the backplate resonance frequencies are not affected much by the damping in case of wafer samples. But the packaged samples are heavily damped and its hard to see the backplate resonance peaks (see Fig.4.11(c)). This is other proof for the influence of air in package. Here also the vacuum measurements provide reliable data about the backplate.

Wafer Sample No	**Resonance in air (kHz)**	**Resonance in vacuum (kHz)**		**Packaged Sample No**	**Resonance in air (kHz)**	**Resonance in vacuum (kHz)**
1	175	181		1	Hard to see	180
2	180	176		2	Hard to see	182
3	181	175				

Table 4.3: Backplate resonance frequencies in air and vacuum conditions measured on wafer and packaged samples (Measurement)

The mechanical resonance frequency extracted can be used to calculate the residual stress in the membrane and the backplate using the Eqn.4.11 [11].

$$f_{nm} = \frac{\omega'_{nm}}{2\pi R}\sqrt{\frac{\sigma}{\rho}} \tag{4.11}$$

where f_{nm} is the frequencies of the Eigen modes, σ is the Stress in Pa, ρ is the density of Si in kg/m^3, R is the radius of membrane/backplate in m and ω'_{nm} is the Eigen-value corresponding to the respective Eigen-mode of the tension dominated plate in which "n and m" represent the number of nodal diameter and nodal circles, respectively. The Eigen values for the lowest twelve Eigen modes are listed in Table.4.4.

(n,m)	(0,0)	(1,0)	(2,0)	(0,1)	(3,0)	(1,1)
ω'nm	2.41	3.83	5.14	5.52	6.38	7.02
(n,m)	(4,0)	(2,1)	(0,2)	(5,0)	(3,1)	(6,0)
ω'nm	7.59	8.42	8.65	8.77	9.76	9.94

Table 4.4: First 12 Eigen modes and Eigen values for a tension dominated plate [11]

The values used in Eqn.4.11 to extract the residual stress in membrane and backplate are, $f_{00,mem}$ = 83 kHz, $f_{00,bp}$ = 170 kHz, R_m = 460μm, R_{bp} = 460μm, ρ = 2301 kg/m^3 and by using the Eigen value for the first Eigen mode (0,0),

the stress calculated in membrane is 23MPa and in backplate 96MPa. These extracted values can be compared with the stress values obtained from finite element simulations [7] to check how well our simulations and reality agrees with each other.

As discussed in Sec.3.3, the theoretical value calculated for the backplate frequency using the initial 180 MPa stress is 215 kHz. The difference between the theoretical and measured frequencies are observed in this electrical measurement as well. This difference is because of the stress variation during processing. Extensive research is going on related to the stress relaxation to identify the exact reason for the mismatch [7].

The membrane stress value (23 MPa) calculated and the Eigen-mode value of 5.52 are used in the same Eqn.4.11 to calculate the first higher mode frequency of the membrane. The first higher mode of the membrane calculated is around 190 kHz. This frequency can be seen in the dissipation Vs frequency vacuum plot at around 200 kHz. This gives a good sign that our theoretical calculations are agreeing with the real device.

Additionally the term Compliance, which is the inverse of Spring Constant, can be calculated from the resonance frequency. Equation4.12 is used for the calculation of membrane compliance.

$$C_m = \frac{1}{2\rho h \pi^3 R_m^2 f_{res}^2(0)} \tag{4.12}$$

4.3 Capacitance – Voltage Measurement

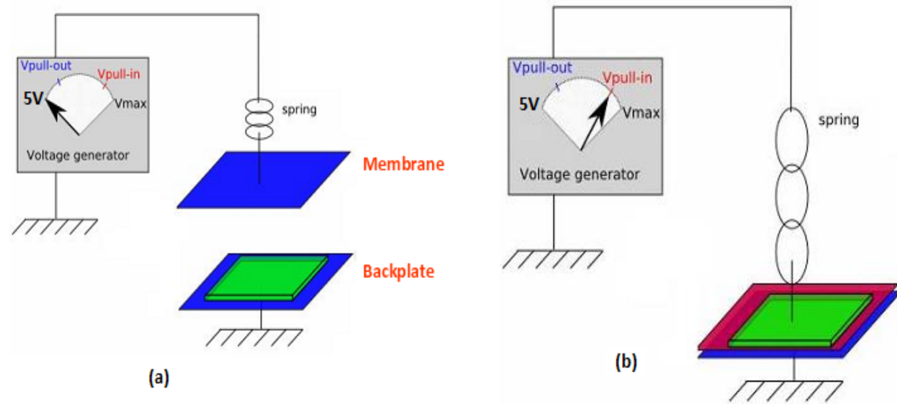

Figure 4.12: (a) Biased stage (5V) of both membrane and backplate and (b) Pull-in voltage stage

As the name states, this measurement is to determine the dependency of the capacitance between the microphone membrane and backplate with respect to the DC bias voltage. This measurement is done at different frequencies by sweeping the bias voltage. In principle this measurement has to be performed when the membrane is stable and its not oscillating. This is possible only

at zero bias voltage, but at zero bias voltage we can't measure the change in capacitance with respect to voltage. In order to perform this measurement an optimal frequency has to be selected where the membrane is stable and there should not be any interference from the resonance frequencies of the backplate.

The DC bias voltage between the membrane and backplate is varied and an AC actuation voltage is superimposed with the bias voltage. Due to the electrostatic force (Eqn.3.1) the membrane is attracted towards the backplate. During the measurement the distance between the membrane and backplate decreases with respect to voltage thus increasing the capacitance. At certain voltage the membrane collapses with the backplate and that voltage is called the Pull-in voltage. When the applied bias voltage is subsequently reduced, the membrane will release eventually from the backplate. The voltage at which the membrane releases back from the backplate is called the Pull-out or release voltage. Fig.4.12 shows the normal stage of the device and the Pull-in stage.

The Pull-in and Pull-out voltages are indicated in the capacitance voltage curve of our device (Fig.4.13). The curve shows the bias voltage is swept from –10V to 10V and back. As stated earlier we can observe the change in capacitance with respect to the bias voltage. Also in the curve the value of capacitance suddenly increases to a value greater than 10pF. The voltage at which the capacitance increases suddenly is the Pull-in voltage and at certain voltage the membrane releases back from the backplate indicating that it is coming out of the Pull-in stage. The voltage at which the membrane releases is called the Pull-out voltage.

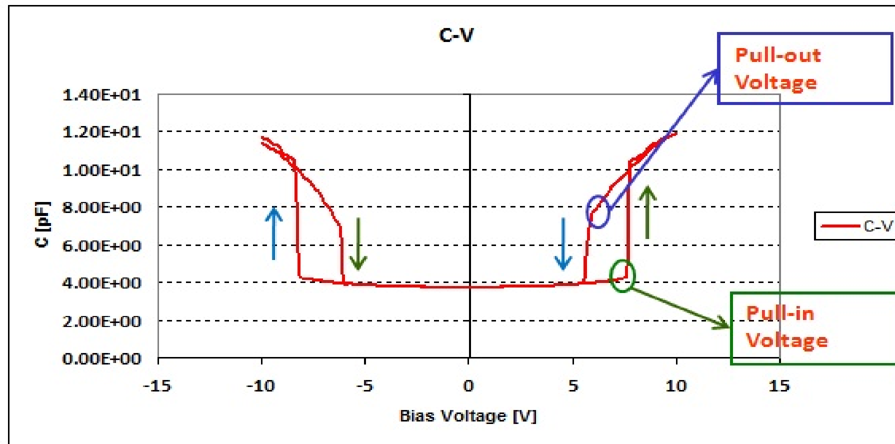

Figure 4.13: Capacitance Vs Voltage plot (Measurement)

4.3.1 Extraction of Membrane Compliance

The extraction of membrane compliance is described here. The Pull – in voltage of NXP MEMS microphones are typically in the order of 7.5V. Eqn.4.13 shows the equation for the Pull – in voltage [11]. This equation can be used to calculate the membrane compliance (C_m) value from the Pull – in voltage and the membrane compliance calculated for 7.5V pull-in is 12 mm/N.

$$V_{pull-in} = \sqrt{\frac{g^3}{2\varepsilon\pi R_m^2 C_m}} \tag{4.13}$$

Another procedure to extract the membrane compliance will be discussed now. The Eqn.4.14 shows the relation between the capacitance and the bias voltage at low voltages. This relation is used to extract the membrane compliance.

$$C(V_{bias}) = C_o + \frac{C_o^2 V_{bias}^2}{4g^2} C_m \tag{4.14}$$

C_0 is the membrane - backplate capacitance without parasitic capacitances C_p which add another constant capacitance to this Eqn.4.14. C_0 is calculated from the plate capacitance formula $C_0 = \frac{\varepsilon_0 \pi R_m^2}{g} = 3.09pF$. The value obtained for the constant from the fit (Fig.4.15) is different from the theoretical value calculated. This is because, the value obtained from measurement has parasitic capacitance included in it.

From the equation it is understood that the relation between capacitance and voltage is a polynomial. This equation is valid only for 60% of Pull – in voltage. In our case 60% of Pull – in is 4.5V. Thus a polynomial plot can be drawn if we zoom into the range of –4.5V to 4.5V. Fig.4.14 shows the plot of that valid range.

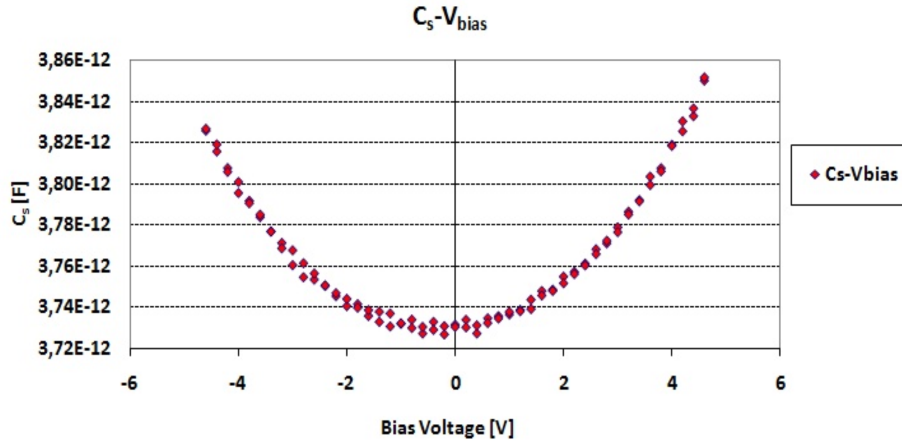

Figure 4.14: Capacitance Vs Voltage plot for the valid range

As expected we have a parabolic behavior in the valid range. In order to extract the compliance value from the data, we need to plot the valid range (60%) V_{bias}^2 Vs C_s. The plot obtained is shown in Fig.4.15. The linear equation obtained from the plot can be related to Eqn.4.14 and the membrane compliance is extracted. The membrane compliance extracted is 6.5 mm/N.

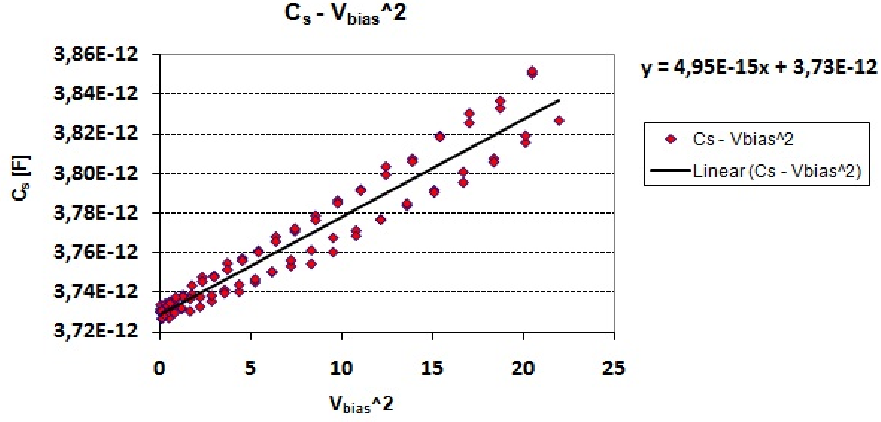

Figure 4.15: Capacitance Vs voltage square plot for the valid range (Measurement)

The error associated with the compliance value is calculated in the same way explained in Sec.4.2.1. The values obtained after applying LINEST function for linear fit is given in Table4.5. Here $a = \frac{C_0^2}{4g^2}C_m$.

$\mathbf{a}$	4.95 x 10^{-15}	$\mathbf{C}_o + \mathbf{C}_p$	3.73 x 10^{-12}
$\boldsymbol{\sigma}_a$	1.41 x 10^{-16}	$\boldsymbol{\sigma}_{C_o+C_p}$	1.39 x 10^{-15}

Table 4.5: LINEST function data of the polynomial fit

The error obtained for membrane compliance using this theory is given in Eqn.4.15 and the statistical error in the membrane compliance is approximately 0.2 mm/N.

$$\sigma_{C_m} = \left(\frac{4g^3}{\varepsilon\pi R_m^2}\right)\sigma_a \tag{4.15}$$

Additionally, the membrane compliance calculated from the pull-in can be compared with the results extracted from the Eqn.4.14. The compliance calculated using the pull-in voltage is 12 mm/N and the extracted values are around 6.5 mm/N. In other words, a factor of two different between the values. The reason for the difference could be that the approximations used for compliance extraction is not much accurate, since it is based on the lumped element model. Also in our Eqn.4.14 the capacitance C_0 is used for a solid plate but in reality the fringing fields due to the perforation in backplate will affect the capacitance between the plates. The drop of capacitance with respect to this perforation level is analyzed by NXP researchers and it is found that a drop of 15% in capacitance for 30% perforation [15]. More analysis has to be done to check and prove this difference since not many literature's are available to cross verify it.

4.3.2 Optimal Frequency selection

As stated earlier, this capacitance voltage measurement is done by sweeping the DC bias voltage at certain frequency. Here the measurement and analysis performed to identify the optimal frequency is discussed. Capacitance voltage measurements are performed on five samples on wafer for different frequency values such as 20 kHz, 200 kHz, 1 MHz and 2 MHz.

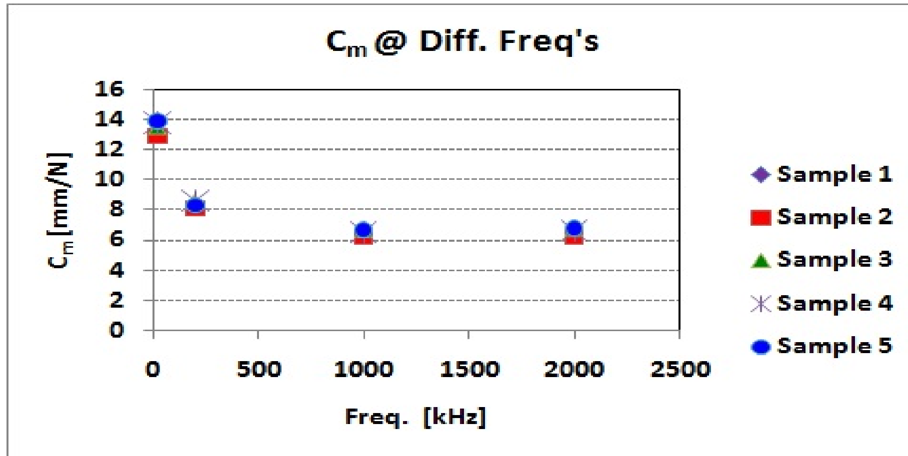

Figure 4.16: Membrane compliance comparison for 2 samples for different frequencies (Extracted)

Fig.4.16 shows the comparison of compliance values extracted for 5 samples at different frequencies. It can be observed from the extracted compliance values, they are high at low frequency and it gradually decreases with increase in frequency and finally it is almost stabilized at high frequencies. This gives us a clear picture of the membrane compliance trend with respect to frequency. The reason for this behavior is that at low frequencies such as 20 kHz, the inertial force of the membrane is small and it will move in accordance with the frequency, which makes the membrane oscillate more, and with increase in frequency it is unable to follow such high frequency and finally it comes to almost stable position. This gives us a situation where the membrane is almost stable and it is the desired condition for the capacitance voltage measurement, which made us to select 1 MHz as the optimal frequency for all the measurements. A further advantage of 1 MHz is that this frequency does not coincide with a resonance of the sensor. At a resonance, the membrane will not be stiff, as desired. Hence, 200 kHz would not be a suitable choice, since this is in near vicinity of both membrane and backplate resonance frequencies Fig.4.11(a). It is not a good idea to rely on the values obtained close to the resonance frequencies.

4.3.3 Influence of AC voltage

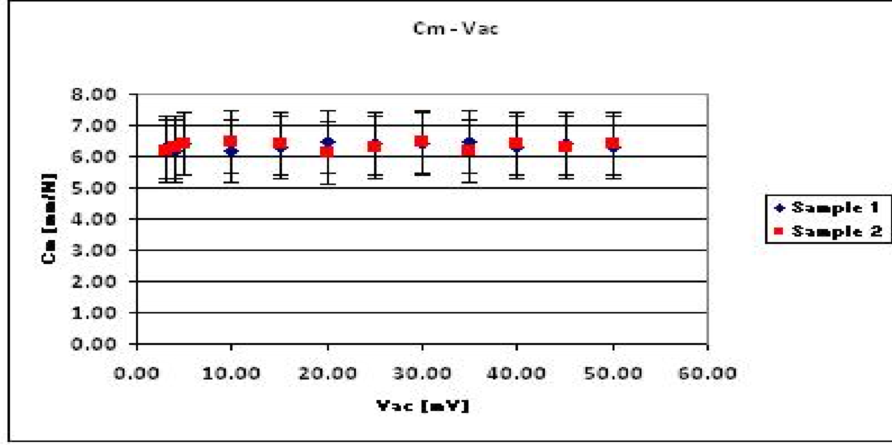

Figure 4.17: Influence of AC voltage on compliance values (Extracted)

This measurement is performed to find the influence of AC voltage superimposed with the DC voltage. This effect has to be analyzed since it is necessary to identify the parameters influencing the resonance frequency and the membrane compliance. Capacitance voltage measurement is performed for different AC voltages from 3mV to 50mV for two different samples and the compliance values obtained are shown Fig.4.17. From the figure it is observed that the influence of AC voltage on the compliance values is negligible and the values agree with each other within the fit error range. This gives us an idea about the choice of AC voltage and now it proves that any value of AC can be selected for our measurements. The AC voltage selected for our measurements is 200 mV.

4.3.4 Membrane compliance in vacuum

Capacitance voltage measurement is performed on packaged MEMS microphones in both air and vacuum conditions by sweeping the DC bias voltage at 1 MHz frequency and the compliance values are extracted. These extracted values are listed in the Table.4.6.

Packaged Sample No	Compliance in air (mm/N)	Compliance in vacuum (mm/N)
1	8.6	7.9

Table 4.6: Membrane compliance values in air and vacuum conditions measured on wafer and packaged samples (Measurement)

From the result listed in Table.4.6 it is observed that the values are different for both air and vacuum measurements. In general, the value should be same in both cases, since we are measuring at 1 MHz and the membrane is assumed to be stable. The reason is unclear for this change in compliance values. In order

to identify the trend, more measurements has to be performed on different packaged samples. With more results, it will be easy to predict or identify the device behavior.

4.4 Summary

In this chapter, the electrical impedance measurement techniques and their measurement setups were discussed. The extraction of resonance frequency and compliance values were shown. Also the results of wafer and packaged samples for both air and vacuum conditions were listed.

First the difference in calibration techniques between different measurement setups were identified. The reason for the difference is because of the degradation of the external standard substrate used for calibration. Finally the open calibration is followed in all the setups and the difference in readings were eliminated.

In case of resonance frequency measurement, series capacitance is used instead of parallel capacitance because of drop in parallel capacitance value at higher frequencies.

From the extracted membrane resonance frequency measurement results (Table.4.2) on both wafer and packaged samples under air and vacuum conditions, the influence of air in the package is identified. The air and vacuum measurement results on wafer matches well but on the other hand the air and vacuum measurements on packaged sample is different. The resonance frequencies measured and the stress values extracted from the resonance frequencies under vacuum conditions matches perfectly with the FEM simulation results. This proves that the vacuum measurement results are reliable and those are the ones to be considered for comparing with FEM simulations.

Finally from the C-V measurements the membrane compliance is extracted and the pull-in voltage of the device is identified. The optimal frequency to perform C-V measurement is identified as 1 MHz. Also the influence of AC actuation voltage over the compliance is found to be none. The membrane compliance values extracted from C-V, calculated from pull-in voltage and membrane resonance frequencies are compared with each other and the differences between the values are analyzed in Chapter.5.

Chapter 5

Measurement Results Comparison and Discussion

In this chapter, results from resonance frequency, compliance and laser vibrometer measurements are compared and discussed.

First the impedance and capacitance - voltage measurements are related to each other by the relation given by Eqn.4.12. This shows us that the membrane compliance values can be calculated from the extracted membrane resonance frequency. This calculated membrane compliance can be compared with the membrane compliance extracted from capacitance - voltage measurement and the membrane compliance calculated from the pull-in voltage. Table.5.1 lists the values obtained from all these techniques on the very same sample.

Membrane compliance from Resonance frequency (80 kHz) (mm/N)	**Membrane compliance from pull-in voltage (mm/N)**	**Membrane compliance from C-V (mm/N)**
13 (Eqn.4.12)	12 (Eqn.4.13)	6.5 (Eqn.4.14)
9.4 (Eqn.5.3)		

Table 5.1: Membrane compliance comparison from different measurements

From the values listed, it can be observed that the membrane compliances from resonance frequency and pull-in voltage are in the same range and the compliance extracted from C-V is different. One reason for this difference is that the approximation used for resonance frequency extraction is not accurate since it is based on a quasi static model (lumped element model); But the shape of the deflection profile changes with respect to frequency. The compliance value calculated from the resonance frequency is static membrane compliance. In order to compare these two values we need to convert the static membrane compliance into dynamic membrane compliance. This can be done by using the conversion factor obtained from the equations described below.

Static membrane compliance is given by [11],

$$C_m \backsimeq \frac{1}{4\pi\sigma_m h_m} \tag{5.1}$$

and the dynamic membrane compliance is given by [11],

$$C_m^{'} \backsimeq \frac{1}{2.89\pi\sigma_m h_m} \tag{5.2}$$

The ratio of static and dynamic obtained is,

$$\frac{C_m^{'}}{C_m} \backsimeq 0.72 \tag{5.3}$$

and this factor is used to convert the static compliance into dynamic compliance. These converted values are listed in Table.5.1 and still the values are different. Furthermore, the extraction of membrane compliance from C-V is at the condition where the membrane is assumed to be stable. But we have seen in Sec.4.3.2 that at lower frequencies or close to resonances the C-V curve is influenced. From Sec.4.3.2 it follows that the error is small for the chosen frequency of 1 MHz. Hence the compliance extracted from C-V is static membrane compliance.

Another factor that could account for this difference is the electrical field distortion (Fringing field) due to the perforation in backplate. As stated earlier, the perforation in the backplate leads to drop in capacitance [15]. This means that the electrostatic force is smaller for a perforated backplate than for a solid one as assumed in the C-V equation (Eqn.4.14). The compliance extracted from C-V is therefore too low.

Another assumption which could have an influence is the fitting range in case of C-V measurement. Now it is stated that the 60% of pull-in is the valid range for compliance extraction. In case if the fitting range is 40% then the value extracted will be different. More analysis and perfect modelling has to be done to understand this difference in depth.

The compliance from pull-in is higher than the other values. The reasons are unclear for the difference in the compliance values. May be the fringing field play a role, since the analytical model assumes a solid plate. In reality the plate is perforated and it deforms with respect to voltage.

From the measurement results listed in Table.5.2 it is identified that the results from vacuum measurements are the ones to be trusted. It matches very well with the FEM simulations (Table.5.2) and provides a good data to compare the stress values extracted from vacuum measurement with the simulation results (Table.5.3).

Resonance in vacuum (kHz) Wafer Sample	**Resonance in vacuum (kHz) Packaged Sample**	**Resonance in calculated (kHz) FEM Simulation [7]**
84 ± 1.0	83 ± 0.7	80
80 ± 0.8	81 ± 0.8	80

Table 5.2: Resonance Frequency extracted from wafer and package samples in vacuum compared with FEM simulation results

Membrane stress extracted (MPa) Wafer Sample (Vacuum)	**Membrane stress extracted (MPa) Packaged Sample (Vacuum)**	**Membrane Stress calculated (MPa) FEM Simulation [7]**
22	24	20
23	23	20

Table 5.3: Membrane stress extracted from membrane resonance frequency for wafer and package samples in vacuum compared with FEM simulation results

In case of stress value comparison between simulation and measurement results, vacuum results gave a good match and this shows that the values obtained are more realistic. But vacuum setup is complicated and it won't be available in all labs. The most available measurement is the C-V measurement. In case of sensitivity it is directly related to compliance and this is measured at the condition where the membrane is stable. It has no influence from resonance frequency and its deflection profiles only if frequency is chosen well.

The laser vibrometer (LV) measurement results can be compared with the resonance frequencies and their higher modes extracted/calculated from impedance measurements. Laser vibrometer gives us a clear picture to visualize the oscillations of the backplate and its fundamental and higher mode frequencies can be measured. Table.5.4 lists the values of backplate resonance frequencies measured in laser vibrometer and the first resonance of backplate measured in electrical impedance and the calculated higher modes using Eqn.4.11 and we can observe that the values deviate from the measured values for the higher modes. One reason for this difference is the bending stiffness of the backplate. Here the equation (Eqn.4.11) used to calculate the higher modes is based only on the stress and the thickness and bending stiffness are neglected. This thickness term and additionally the material properties like Young's modulus will have some influence on the resonance frequency which leads to increased higher mode frequencies due to the added forces from the bending.

Production sample	**From laser vibrometer measure-ment (kHz)**	**From impedance measure-ment (kHz)**
f_{00}	189	182 (Measured)
f_{01}	460	415 (Calculated)
f_{02}	780	650 (Calculated)

Table 5.4: Backplate resonance frequency and higher mode frequencies comparison between Laser vibrometer and electrical impedance

Another measurement performed using laser vibrometer on packaged sample can be compared with the impedance measurements of packaged samples in air. When we compare the laser vibrometer results (see Fig.3.14 and Fig.3.15) with Fig.4.11(c), the presence of the peak at around 25 kHz is visible in both results and the complete frequency spectrum agree with each other quiet well.

It can be hoped that the laser vibrometer enables new measurements in the future to gain more understanding of the device mechanics. For example, the low frequency measurements performed to analyze the displacement (Fig.3.13) can be extended to extract the electrostatic force.

Chapter 6

Conclusions and Recommendations

6.1 Conclusions

The work presented in this report focused on the investigation and comparison of different measurement principles and techniques used to measure the key device parameters, resonance frequency and compliance. The influence of ambient pressure, bias voltage and back volume on the resonance frequencies were analyzed. The performance limiting factor called body noise was introduced and the techniques to avoid it was shown. One key technique to eliminate body noise is the frequency matching. Hence it becomes obvious to measure and analyze the resonance frequency of the membrane and backplate. Additionally the compliance term which is related to the sensitivity of the device was also measured and analyzed.

Electrical impedance measurements provide us details about the influence of bias voltage over the resonance frequency and the influence of air in the package by comparing the air and vaccum results. Also the influence of the electrode resistance at higher frequencies is proved by the drop in C_p. C_s is then a better choice. Additionally from the comparison of two different setups used for electrical impedance measurements, it is identified that the calibration techniques were different which results for the mismatch between them. With the common open calibration in both setups resulted for the agreement of readings. Hence open calibration is followed for all the electrical impedance measurement as the least error-prone calibration. From the results of the electrical impedance measurements it is identified that the vacuum measurement results are more reliable and it gives info purely related to membrane and backplate. The capacitance voltage measurements provided the pull-in voltage of the device and the membrane compliance extracted was compared with other measurement readings and the mismatch was analyzed. Also the optimal frequency for C-V measurement is identified as 1 MHz and the influence of AC actuation voltage over the membrane compliance is found to be none.

Laser vibrometer measurements provided us with details about the operation of the device especially the deflection profiles and the resonances were easily identified. From the difference between measured and calculated higher

mode resonance frequencies, it is concluded that the influence of the bending stiffness of the backplate and other material properties like Young's modulus are not negligible. The stress values extracted from the measured fundamental resonance frequencies are in good agreement with FEM simulations. The normal 2X and 50X magnification measurements provides us with details about the difference between the magnifications. The problem with the 2X magnification measurement is identified as being influenced by both membrane and backplate movement. The 2X magnification should therefore be used to measure qualitative mode shapes. In case of 50X magnification measurement it focuses the scanning surface very accurately and it gives the pure readings of the subject. This shows that the reading obtained from 50X is the one to trust. However, the 50X magnification does not allow to scan the displacement profile over the full backplate.

It has been shown that laser vibrometer and electrical impedance measurements are related to each other and the results obtained are in the same range. This is important as electrical measurements take less effort and equipment, while the laser vibrometer measurements are direct measurements of the mechanical movement.

6.2 Recommendations

Some recommendations can be pointed out to extend the work performed here. In case of laser vibrometer measurement only the electrical measurements were performed. Additionally mechanical actuation is possible by placing the sample over a shaker. This helps to visualize/determine the asymmetric mode shapes of the circular membrane/backplate which can then be compared with the calculated values. Also the measurement performed for displacement can be extended to extract the electrostatic force, if proper equations are derived.

In case of electrical impedance measurement, the equations used for compliance extraction should be modified including the effects of fringing field. In spring suspended backplate design, the resonance frequency is tunable by the number and properties of springs and the desired frequency range can be reached. The most important next step is to process a full sensor with a spring suspended backplate. Measurement of resonance frequencies of spring suspended backplates can be performed to check the reduction in the body noise. This is the most important value of the sensor and a detailed analysis and measurements have to be performed. The mechanical stability of the suspension is an important point which needs to be investigated.

Bibliography

[1] G. Meijer, *Smart Sensor Systems.* WILEY, 2008.

[2] P. French, *Silicon Sensors.* Delft University of Technology, 2009.

[3] Electronics Advocate, "Mems microphone market," February 2010. [Online]. Available: http://www.electronicsadvocate.com/wp-content/uploads/2010/02/isupplimemsmarket.jpg

[4] Wikipedia, "Microphone," April 2010. [Online]. Available: http://en.wikipedia.org/wiki/microphone

[5] F. S. Consulting, "Silicon mems microphone market set to grow strong, says the information network," March 2010. [Online]. Available: http://futuresource.trackandmonitormedia.com/?p=32638

[6] Design News, "Tiny mems microphone boosts audio quality," September 2009. [Online]. Available: http://www.designnews.com/article/339420-Tiny_MEMS_Microphone_Boosts_Audio_Quality.php

[7] A. F. V. Quintero, ""master thesis - stress evolution of functional layers inmems devices throughout the processing"," 2010.

[8] R. Jaeger, *Introduction to Microelectronic Fabrication*, 2nd ed. Prentice Hall, 2002.

[9] Paul Mcwhorter, "About mems," May 2009. [Online]. Available: http://www.memx.com/

[10] F. Felberer, "Master thesis - characterisation of mems microphones for body noise," 2009.

[11] I. Bominaar-Silkens, NXP Semiconductors, Tech. Rep., 2009, in preparation.

[12] G. Langereis, "Microphone models for body-noise cancellation," NXP Semiconductors, Tech. Rep. NXP-R-TN 2008/00313, 2008.

[13] M. Goossens, "The polytec laservibrometer:measuring mems movements on the nano scale," February 2010. [Online]. Available: http://nww.nxp.com

[14] Wikipedia, "Electrical impedance," May 2010. [Online]. Available: http://en.wikipedia.org/wiki/Electrical_impedance

[15] G. Langereis, "A lumped element model for mems microphones," NXP Semiconductors, Tech. Rep. PR-TN-2005/00209, 2005.

Appendix A

Influence of calibration techniques on the extracted results

Membrane compliance values extracted for 5 samples measured in both Multifrequency RLC meter and Impedance Analyzer are listed in Table.A.1. This measurement is performed with old calibration technique and the influence of the calibration can be observed in the results. The results are different for same samples measured in different setups under same conditions.

Sample No	Multifrequency RLC meter (mm/N)	Impedance Analyzer (mm/N)
1	6.4	8.5
2	6.2	8.7
3	7.0	8.4
4	6.5	8.9
5	6.7	9.1

Table A.1: Compliance values for 5 samples from different measurement setups

Table.A.2 shows the membrane compliance values extracted for 5 samples in different setups under new open calibration technique. It can be observed that the results are matching with each other and this open calibration technique is followed for all other measurements.

Sample No	**Multifrequency RLC meter (mm/N)**	**Impedance Analyzer (mm/N)**
1	6.4	6.6
2	6.2	6.4
3	7.0	6.8
4	6.5	6.6
5	6.7	7.0

Table A.2: Compliance values for 5 samples from different measurement setups after new calibration

Appendix B

10 cycles with same conditions (2X)

DC Voltage = 5V, AC voltage = 0.5 V, Vibrometer range = 500mV, Freq. Range = 0 to 200 kHz

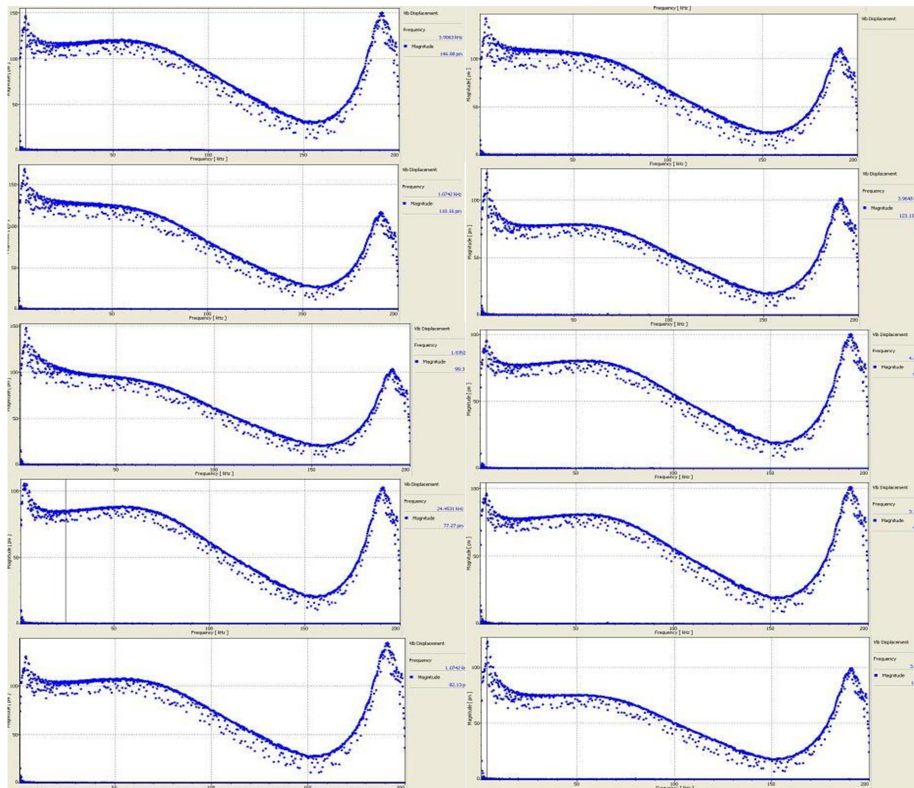

Figure B.1: Ten measurements for the same conditions for same sample to check the reproducibility of the measurement

Measurement for changing vibrometer range

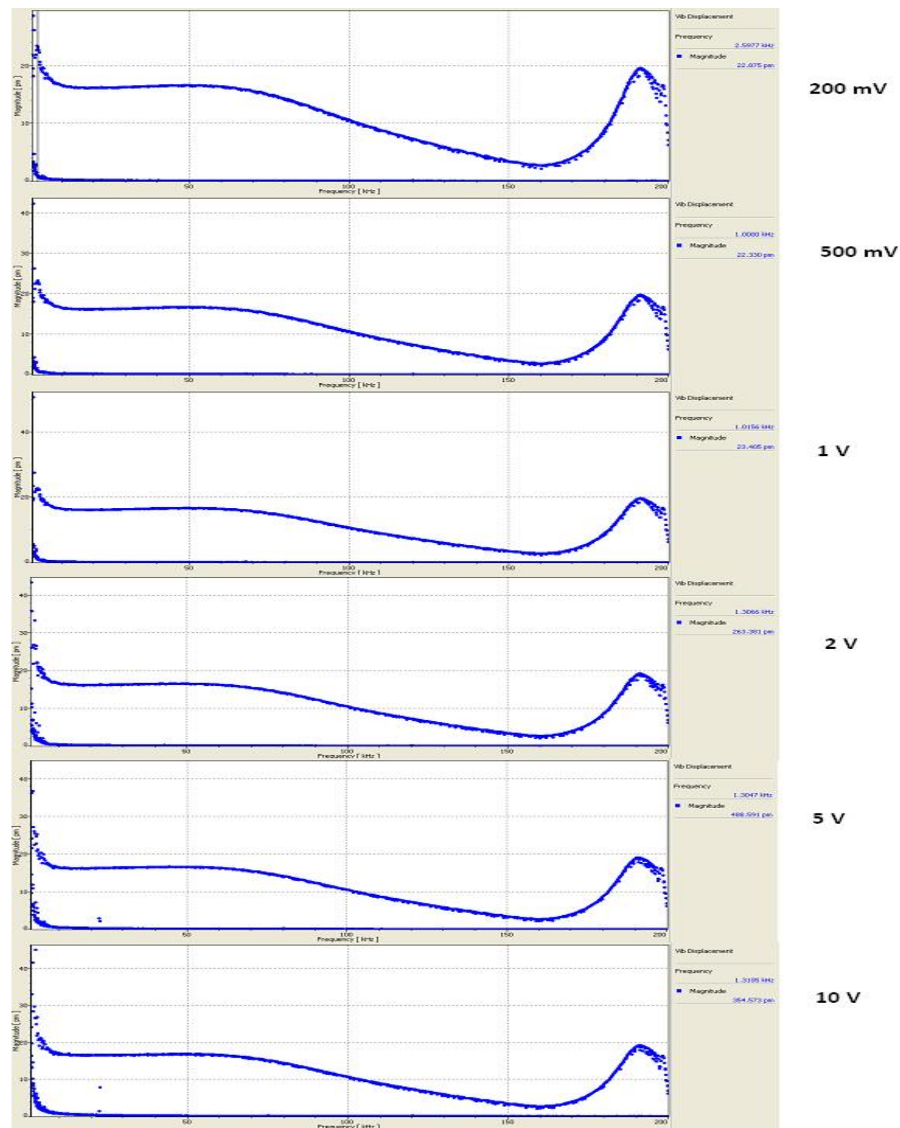

Figure B.2: Measurements for the same conditions for same sample to check the influence of the vibrometer range